2014

Conformational Regulation of Membrane Localization and Activation of Talin

Pallavi Dwivedi
Cleveland State University

CONFORMATIONAL REGULATION OF MEMBRANE LOCALIZATION AND ACTIVATION OF TALIN

PALLAVI DWIVEDI

Master of Biochemistry

Panjab University

July, 2008

Submitted in partial fulfillment of requirements for the degree

MASTER OF SCIENCE IN BIOLOGY

at the

CLEVELAND STATE UNIVERSITY

May, 2014

We hereby approve this thesis for

Pallavi Dwivedi

Candidate for the Master of Science in Biology degree for the

Department of Biological, Geological & Environmental Sciences

and the CLEVELAND STATE UNIVERSITY

College of Graduate Studies

Thesis Chairperson, Dr. Jun Qin

Department of Molecular Cardiology, Lerner Research Institute
Department & Date

Thesis Committee Member, Dr. Barsanjit Mazumder

Department of Biological, Geological and Environmental Sciences
Department & Date

Thesis Committee Member, Dr. Sadashiva Karnik

Department of Molecular Cardiology, Lerner Research Institute
Department & Date

May 1st, 2014

ACKNOWLEDGEMENTS

A special word of thanks to my research advisor Dr. Jun Qin for his support, guidance, constructive criticism and constant willing cooperation. I would like to thank my thesis research committee members Dr. Sadashiva Karnik and Dr. Barsanjit Mazumder for their useful and valuable suggestions and encouragement.

I am thankful to Dr. Jun Yang for NMR experiments and teaching me the preparation of MLVs and Dr. Julia Vaynberg for assisting in actin experiments. I am also thankful to Dr. Jamila Hirbawi (Dr. Ed. Plow's lab) for cell based studies. I would like to thank all my other colleagues in Dr. Jun Qin's lab for their helpful suggestions and providing a good lab environment.

I would like to express my gratitude to the Department of Biological, Geological and Environmental Sciences, Cleveland State University and the Department of Molecular Cardiology, Lerner Research Institute (CCF) for giving me an opportunity to work on my research project as a graduate student.

I am thankful to my parents and my husband for their love, understanding and unrelenting support.

CONFORMATIONAL REGULATION OF MEMBRANE LOCALIZATION AND ACTIVATION OF TALIN

PALLAVI DWIVEDI

ABSTRACT

Talin is a cytosolic protein which is known to be one of the key players involved in integrin mediated cell adhesion dependent processes, including blood coagulation, tissue redmodeling. It connects the extracellular matrix with the actin cytoskeleton. Talin comprises of a head domain (talin-H) and a rod domain (talin-R). Talin-H is further subdivided in F0, F1, F2 and F3 domains. Talin-R contains 13 contiguous helical bundle domains (R1-R13) followed by an actin binding dimerization domain (DD). The F3 domain contains a key integrin binding site that regulates integrin activation. In our previous studies, we have shown that cytosolic talin exists in an autoinhibited state where the integrin binding site in F3 domain is self-masked by R9 domain. The autoinhibited talin is randomly distributed in the cytosol but upon activation, talin is rapidly localized to membrane and it binds and activates integrin. The main focus of the present study was to understand the mechanism of plasma membrane localization and activation of talin. Since talin has long been known to also bind to actin, we also investigated the actin binding sites in talin and how they are conformationaly regulated.

The crystal structure of autoinhibited talin F2F3-R9 complex, previously determined in our lab, revealed a stretch of negatively charged residues on R9 which is located on the same side as the positively charged surface on talin H. This leads to two hypotheses: (I) Electrostatic repulsion between the negatively charged talin-R9 surface and membrane promotes the cytosolic retention of autoinhibited talin; (II) upon enrichment of membrane with negatively charged phosphatidylinositol-4,5-bisphosphate (PIP2), PIP2 strongly pulls the positively charged surface on talin-H towards membrane and simultaneously repels the negatively charged surface on R9, thus promoting the membrane localization and activation of autoinhibited talin via a "pull-push" mechanism. To test the hypothesis I, we made a triple mutant (H1711E, T1812E, N1815E) on the talin-R9 (talin-3E mutant) to make it more negatively charged. Our cosedimentation experiment demonstrates that the talin mutant has significantly reduced ability to associate with membrane as compared to the WT talin, thus supporting the hypothesis I. To test the hypothesis II, we made a triple mutant (D1676R, E1770K, M319A) to weaken the talin-F3/R9 autoinhibitory interaction (talin-activation mutant). The co-sedimentation experiment demonstrates that the talin-activation mutant had substantially increased capacity to bind to membrane as compared to WT talin, indicating that the relief of the autoinhibition promoted the "pulling" of talin-H to membrane and "pushing" away of talin-R from membrane. Consistently, the talin-activation mutant had increased integrin-binding, leading to significantly enhanced talin-mediated integrin activation as compared to WT talin.

Consistent with previous studies, we found the presence of three actin binding sites on talin. Interestingly, full length talin has little binding to actin, suggesting that the

full length talin adopts a conformation that not only prevents integrin binding but also the actin binding. Disruption of the autoinhibitory interface that masks the integrin binding increased the talin binding to integrin but not to actin, suggesting that the two binding events are regulated by different conformational activation mechanisms.

TABLE OF CONTENTS

Page

LIST OF FIGURES

Page

NOMENCLATURE

PIP2: Phosphatidylinositol-4,5-bisphosphate

POPS: 1-palmitoyl-2-oleoyl-sn-glycero-3-[phosphor-L-serine]

POPC: 1-palmitoyl-2-oleoyl-sn-glycero-3-phosphocholine

MLV: Multilamellar vesicle

CHO: Chinese Hamster ovary

NMR: Nuclear Magnetic Resonance

HSQC: Heteronuclear Single Quantum Correlation

PTB: Phosphotyrosine Binding domain

DD: Dimerization domain

FERM: 4.1 protein, Ezrin, Radixin, Moesin domain

EGFP: Enhanced Green Fluorescent protein

cDNA: complementary DNA

CT : Cytoplasmic tail

FL : Full length

CHAPTER I

INTRODUCTION

1.1 Integrins

Integrins are heterodimeric transmembrane glycoprotein receptors comprising two subunits α and β which are noncovalently associated with each other. Integrins serve as a mode of interaction of cells with the extracelluar matrix. These receptors play a vital role in cell adhesion and migration. Till date 18α and 8β subunits are known in vertebrates which form 24 distinct integrin receptors which possess different binding properties and are differentially expressed in various tissues (Johnson et al, 2009). For instance, αιιb subunit pairs up with subunit β_3 to form a heterodimeric receptor $\alpha_{IIb}\beta_3$ in platelets which recognizes Arg-Gly-Asp (RGD) peptides in extracellular matrix molecules such as fibrinogen and vitronectin.

Both α and β subunits contain a large extracellular domain, a single membrane spanning transmembrane domain and cytoplasmic tail (figure 1). The extracellular domain of α subunit comprises of inserted domain or von Willebrand factor A domain

(Lee at al.,1995), β propeller domain (Springer et al.,1997) and leg or stalk comprising of thigh domain and calf1 and calf 2 domains (Xiong et al.,2001; Zhu et al.,2008).

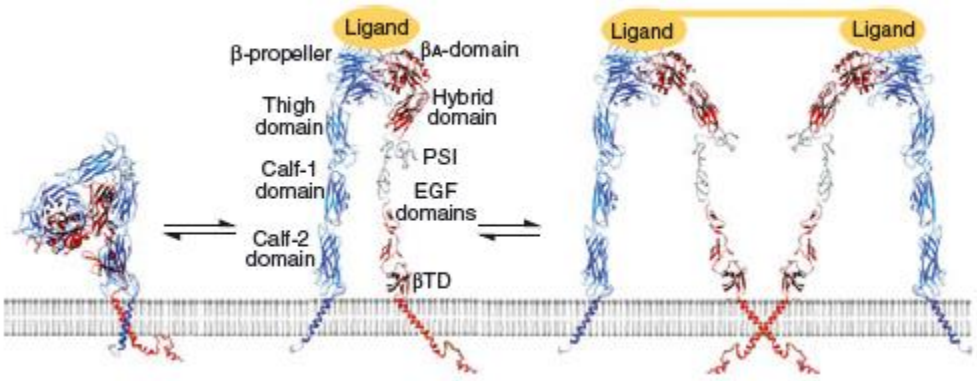

Figure 1 Integrin $\alpha_{IIb}\beta_3$: Integrins are heterodimeric receptors comprising of α and β subunits. The extracellular domain of α_{IIb} comprises of β-propeller domain, the thigh domain , calf-1 and calf-2 domains. The extracellular portion of β_3 subunit comprises of βA domain, hybrid domain, PSI (plexin/semaphorin/integrin) domain, four EGF domains (Epidermal growth factor-like domains) and a β TD domain. The figure shows the 'bent' or inactive form of integrin and 'extended' or active form of integrin which is capable of binding to it's ligand (adapted from Ma et al., 2007)

The inserted domain contains α helices contains a dinucleotide binding or Rossmann fold and it also contains a metal ion dependent adhesion site (MIDAS) which is important for binding to ligand. The β propeller domain forms an interface with the β subunit. The bent or low affinity state of integrins has been suggested to undergo a conformational rearrangement and extension with a switch blade like motion upon inside out signaling and binding binding to a ligand (Takagi et al., 2002; Xiong et al., 2002; Luo et al.,2007; Xiao et al.,2004). The 'genu' or the key point where switchblade like rearrangement

occurs in α subunit is formed by a calcium ion binding loop present between thigh and calf 1 domains of α subunit.

The extracellular domain of β subunit comprises of inserted domain or β_A domain, hybrid domain, Plexin/semaphorin/integrin (PSI) domain and leg or stalk which contains integrin epidermal growth factor like domain (IEGF) and β ankle and αβ tail domain (Shi et al., 2005). The inserted domain of β subunit forms an interface with β propeller of α subunit and like inserted domain of α subunit, it also contains MIDAS which binds magnesium ion and an additional metal ion binding site known as Synergistic metal ion binding site which binds calcium ion (Huang et al., 2000). The 'genu' or bent in the β subunit has been suggested to occur between I-EGF domains 1 and 2. The structure of the extracellular domain of $\alpha_{IIb}\beta_3$ in the ligand bound state and inserted domain of β subunit of $\alpha_v\beta_3$ in absence of ligand suggests that rearrangement of extracellular domain from closed to open conformation occurs following disruption of the interface between inserted domain of β subunit and hybrid domain. The rearrangement of residues in MIDAS and axial displacement of α7 helix of inserted domain leads to swinging out of hybrid domain of β subunit thereby disrupting it's interface with inserted domain.

As revealed in the structure of integrin $\alpha_{IIb}\beta_3$, there is an association between transmembrane domains of α_{IIb} GXXXG motif and β_3 subunit in bent conformation (Xiong et al., 2001; Zhu et al., 2009). Also, the studies on cytoplasmic domains of α and β subunits using FRET (Fluorescence Resonance Energy transfer) have suggested that in resting state the cytoplasmic tails are close to each other and show spatial separation upon binding of talin head domain or phorbol ester (Kim et al., 2003). The disruption of the association of transmembrane and cytoplasmic domains of α and β subunits by making

mutations in specific residues has been shown to activate integrins (Luo et al., 2004; Partridge et al., 2005; Luo et al., 2005).

Integrins have been shown to work as bidirectional signalling receptors (Hynes et al., 2002). Agonist stimulation leads to signalling response within cells and recruitment of signaling proteins onto the integrin α and β cytoplasmic tails which in turn results in activation of integrins. This process is known as inside-out signalling. The formation of a large signaling complex known as focal adhesion takes place in response to binding of a ligand to intgerins. The focal adhesion complex comprises of integrins clustered within the plasma membrane and signaling molecules assembled onto the cytoplasmic tails of integrins. This process is referred to as outside-in signalling (Abram et al., 2009).

1.2 Talin

Talin was initially identified as a cytoskeletal protein which localises in adhesion plaques in ruffling membranes of fibroblasts (Burridge et al., 1983), myotendinous junctions of skeletal muscles (Tidball et al., 1986) and in platelets (Fox et al., 1985). Later studies identified integrins and vinculin as binding partners of talin in cells (Burridge et al., 1984). Talin comprises of N-terminal FERM (protein 4.1, Ezrin, radixin

and moesin) domain-like talin head domain and C-terminal rod domain (figure 2). The head domain is further subdivided into F0, F1, F2 and F3 domains. The talin rod domain is composed of a series of helical bundle subdomains followed by a carboxyl terminal dimerization domain (DD) (figure 2).

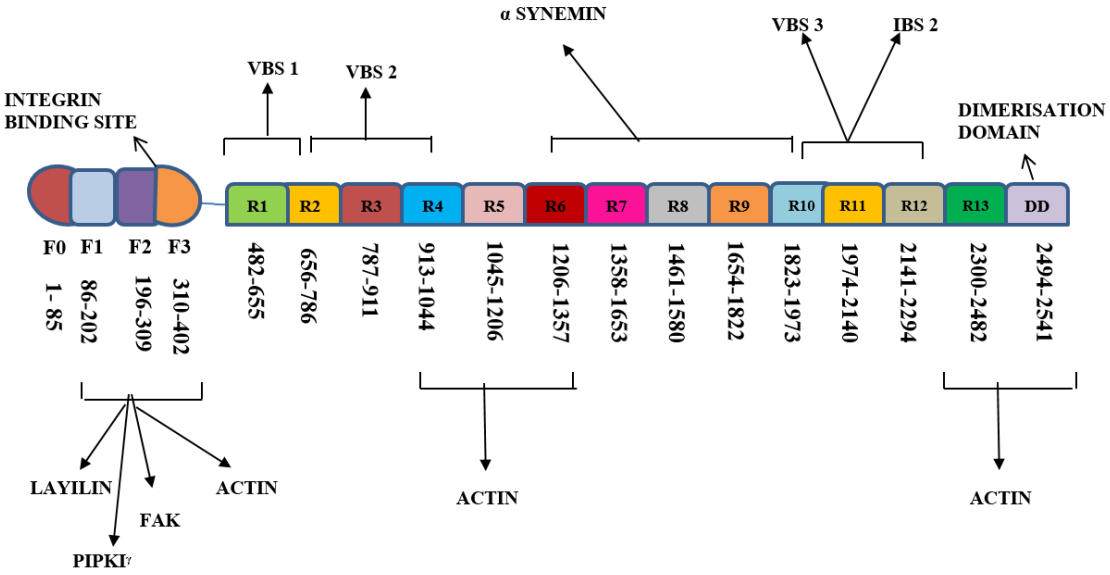

Figure 2 Talin comprises of a head domain and a rod domain. The head domain is subdivided into F0, F1, F2 and F3 subdomians. The rod domain is further subdivided into 13 helical bundle subdomains R1 (482-655), R2 (656-786), R3 (787-911), R4 (913-1044), R5 (1045-1206), R6 (1206-1357), R7 (1358-1653), R8 (1461-1580), R9 (1654-1822), R10 (1823-1973), R11 (1974-2140), R12 (2141-2294), R13 (2300-2482) and DD (2494-2541) followed by carboxyl terminal dimerization domain (DD). The F3 subdomain contains the integrin binding site (IBS 1) which is responsible for activating integrins. F2 and F3 subdomains also contain binding sites for PIPKIγ, Layilin, Focal adhesion kinase (FAK) and actin. The rod domain contains binding sites for actin and vinculin (VBS; vinculin binding sites), α-Synemin and second integrin binding site (IBS2).

The F3 subdomain has a Phosphotyrosine binding fold (PTB) which binds to membrane proximal NPXY motif in the cytoplasmic tails of β subunit of integrin (figure 3, 4). Both F2 and F3 domains of talin have been shown to bind β_3 tail in in-vitro studies using Surface Plasmon Resonance (SPR). Talin F3 binds integrin β_3 tail with much higher affinity (Kd 130 ± 10nm) as compared to F2 domain (Kd 540 ± 40 nm).

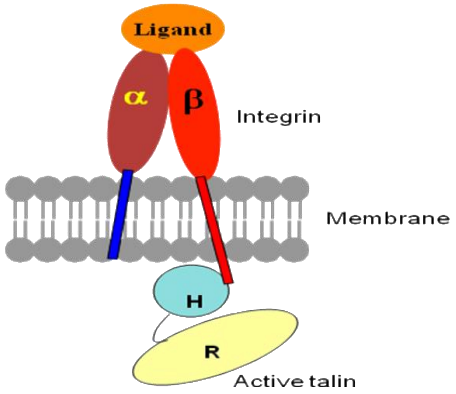

Figure 3 The F3 subdomain of activated talin head domain activates integrin by binding to the cytoplasmic tail (CT) of β subunit of integrin.

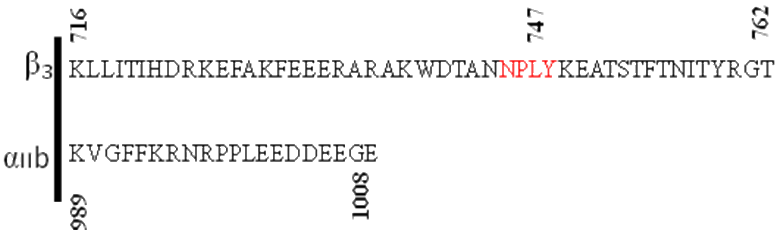

Figure 4 Talin binds to NPXY motif (shown in red) in β_3 CT of integrin $\alpha_{IIb}\beta_3$.

The binding affinity of talin head domain (Kd 91 nm) is similar to that of the F3 domain. Talin has been shown to bind β_3, β_1D tails and also weakly to β_1 A tail (Calderwood et al., 1999; Calderwood et al., 2002). In previous NMR studies, the residues 732-750 corresponding to NPXY motif showed largest spectral changes in full length integrin β_3 tail in presence of talin fragment encompassing F2 and F3 domains (Vinogradova et al., 2002; Vinogradova et al., 2004; Ulmer et al., 2003).

Upon cotransfection with talin 1-1071 fragment cDNA, Chinese hamster ovary (CHO) cells expressing integrin showed increased activation of integrin as monitored by activation specific monoclonal antibody PAC1. On the other hand cotransfection of these cells with talin fragment (434-1071) lacking head domain could not activate integrin. Also, the expression of talin (1-1071) in CHO cells expressing integrin $\alpha_{IIb}\beta_3$ lacking C-terminal 35 amino acids of β_3 tail fails to activate integrin and cause cell spreading and formation of focal adhesions (Calderwood et al., 2002; Calderwood et al., 1999). The interaction of talin with integrin is also disrupted by point mutation of tyrosine (Y) in the NPXY motif to alanine (A).

The binding of talin to membrane phosphoinositides facilitates its interaction with integrin β cytoplasmic tails (Martel et al., 2001). The FERM domain of talin contains a stretch of positively charged residues which aids interaction of talin with negatively charged phosphoinosites in membrane (Kalli et al., 2013). PIPKIγ, which locally enriches membrane with PIP2, also binds to FERM domain of talin and is recruited to membrane by talin (Ling et al., 2002; Paolo et al., 2002). PIP2 has been shown to activate talin (Goksoy et al., 2008). Previous studies have suggested that

binding of PIP2 to talin sterically induces conformational change in talin and leads to its activation (Martel et al., 2001).

Talin acts as linker between extracellular matrix and actin cytoskeleton. Disruption of both talin alleles in mouse embryonic stem cells leads to inability to complete gastrulation and embryonic lethality in mice (Monkley et al., 2000). The defects in talin deficient mouse embryos have been suggested to occur due to defects in assembly of focal adhesions and cell spreading (Priddle et al., 1998). Also, downregulation of expression of talin in HeLa cells using antisense RNA strategy leads to decrease in number of stress fibers and reduced rate of cell spreading (Albiges-Rizo et al., 1995).

Fusion proteins spanning the residues 102-497, 951-1327 and 2269-2541 of talin have been shown to bind F-actin in *in vitro* cosedimentation assay (Hemmings et al., 1996). These studies suggest the presence of atleast three distinct actin binding sites on talin. F2 and F3 subdomains of talin head domain have been shown to colocalize with actin stress fibers in COS cells and cosediment with F-actin in invitro studies (Lee et al., 2004). These findings suggest that the FERM domain of talin head contains the actin binding site and both F2 and F3 subdomains of actin contribute to binding to actin. The interaction of talin with actin has been shown to be affected by change in pH and ionic strength and temperature (Schmidt et al., 1999). Also, using high resolution electron microscopy the binding site of talin FERM domain has been mapped to subdomain 4 of an actin monomer (Gingras et al., 2008).

The structure of COOH-terminal actin binding domain shows resemblance to HIP1R THATCH (talin/ HIP1R/ Sla2p actin tethering C-terminal homology) core domain or I/LWEQ motif (Brett et al., 2006; Gingras et al.,2008; McCann et al., 1997). The core of

this domain is formed by five helix bundle spanning the residues 2300-2482. The bundle is linked to helix 6 which forms an antiparallel dimer. The dimerisation helix is required for binding of talin to F-actin. The helix 1 which lies on the opposite side of the five helix bundle negatively regulates binding to F-actin. The N terminal and C terminal actin binding sites of talin have been suggested to exhibit different characteristics (Hemmings et al., 1996). Upon microinjection into chicken embryo fibroblasts talin GST fusion protein spanning residues 102-497 and 1646-2541 caused disruption of actin stress fibers. The fusion protein containing the C terminal actin binding site spanning residues 1646-2541 could not disrupt actin stress fibers (Bolton et al., 1997).

1.3 Binding Partners of Talin

Talin contains an integrin binding site on FERM domain (figure 2) as well as on the rod domain (Calderwood et al., 2002; Moes et al., 2007). The integrin binding site on the head domain of talin is responsible for activating integrin. The head domain also binds to a splice variant of phosphatidylinositol-4-phosphate 5 kinase (PIPKIγ90) (Paolo et al., 2002) and membrane phospholipids (Martel et al., 2001; Kalli et al., 2013). Talin has been shown to contain three vinculin binding sites VBS1 (498-636), VBS2 (727-965) and VBS3 (1943-2157) in the rod domain (Bass et al., 2002). The crystal structure of talin 482-789 has been determined. A five helix bundle formed by residues 482-655 forms a

hydrophobic interface with four helix bundle formed by residues 656-789. The hydrophobic residues L608, A612, L615, V619 and L623 form vinculin binding site in talin rod domain. Mutations that disrupt the hydrophobic core have been shown to expose vinculin binding site in talin. These studies suggest that talin 482-655 requires activation in order to bind vinculin.

A 48 amino acid sequence spanning the residues 965-1012 in the carboxyl domain of Focal adhesion kinase (FAK) has been shown to bind talin in NIH3T3 cells. The binding site of FAK on talin comprises of residues 225-357 within talin's FERM domain (Chen et al., 1995; Borowsky et al., 1998). The binding of cytoplasmic domain of integrin to talin has been suggested to lead to the activation of FAK and tyrosine phosphorylation. Layilin has also been identified as a binding partner of talin in yeast two hybrid screen. It has been named Layilin due to the sequence LAYILI in it's transmembrane domain. Layilin has a 130 amino acid domain which is homologous to C-type lectin carbohydrate recognition domain. The amino acids 280-435 constitute the binding site for Layilin on Talin (Borowsky et al., 1998). Another binding partner of talin, α Synemin is a member of the intermediate filament protein family. Synemin colocalizes with talin in mammalian muscle cells at sites of focal adhesion. α Synemin contains a 312 amino acid insert (SNT III) which binds to rod domain of talin (Sun et al., 2008). Talin has been shown to bind actin (Hemmings et al., 1996; Lee et al., 2004).

1.4 Aim of the Project

The head domain of talin (Talin-H) activates integrin by separating a key cytoplasmic clasp of integrin α and β subunits (Kim et al., 2003). The stretches of positively charged surfaces on talin-H have been suggested to facilitate interaction of talin-H with integrin β cytoplasmic tail by promoting binding of talin to plasma membrane (Kalli et al., 2013). We found that rod domain of talin specifically talin-R9 sterically blocks the integrin membrane proximal β cytoplasmic tail site on talin-F3 (Goksoy et al,2008). This finding explains how conformational regulation of talin in turn regulates talin mediated integrin activation. However, the following questions still remain unaddressed:

1. How is talin retained in the cytoplasm? Talin has long been known to be randomly distributed in cytosol in resting cells. However, the mechanism which determines the cytosolic retention of talin so that it is incapable of binding to integrin is unknown.
2. How is talin localized to the membrane and activated to bind integrin? PIPKIγ kinase, recruited by talin to the membrane enriches membrane with PIP2. PIP2 has been shown to promote talin mediated integrin activation (Goksoy et al., 2008). However, how does PIP2 help in localization of talin to the membrane and it's activation is not well understood (Song et al., 2012).

3. How is the interaction of talin with actin regulated? Talin has long been known to act as a linker between extracellular matrix and actin cytoskeleton at sites of cell adhesion to substrate. Previous studies have indicated the presence of multiple sites on talin. However, the mechanism which regulates the interaction of talin with actin and which of the previously reported actin binding sites in autoinhibited talin are available to bind to actin in resting cells remains unclear.

Our crystal structure of Talin F2F3/R9 autoinhibitory complex (figure 4; Song et al., 2012) revealed a stretch of negatively charged residues on rod domain of talin which is located on the same side as the stretch of positively charged residues on talin F2F3. Based on this finding I propose the following studies to address the above questions.

1. Test the hypothesis that electrostatic repulsion between the negatively charged talin-R9 surface and membrane promotes the cytosolic retention of autoinhibited talin. We will use lipid cosedimentation assay to compare the binding abilities of purified talin fragments F2F3, F2DD , FL talin and FL mutant (H1711E, T1812E, N1815E), R1-R9, R9 (figure 2) to MLVs (multilamellar vesicles) enriched with lipids found on the inner surface of plasma membrane such as PIP2 (Phosphatidylinositol-4,5-bisphosphate), POPS (1-palmitoyl-2-oleoyl-sn-glycero-3-[phosphor-L-serine]) and POPC (1-palmitoyl-2-oleoyl-sn-glycero-3-phosphocholine). To determine whether localization of FL talin and FL talin mutant (T1767L, E1770K, M319A) to membrane also affects the ability of these proteins to activate integrin, we will use integrin activation assay in CHO cells. The integrin activation assay is based on analyzing the binding of the

monoclonal antibody PAC1 which specifically binds to activated integrins using FACS (Fluorescence activated cell sorting).

2. Test the hypothesis that upon enrichment of membrane with negatively charged PIP2, PIP2 strongly pulls the positively charged surface on talin-H towards membrane and simultaneously repels the negatively charged surface on R9, thus promoting the membrane localization and activation of autoinhibited talin via a ”pull-push” mechanism. We will use lipid cosedimentation assay to compare the binding ability of purified talin fragments F2R9 and F2R9 mutant (D1676R, E1770K, M319A) to MLVs enriched in varying concentrations of PIP2 (5-20%). The assay will help us determine how the weakening of autoinhibitory F2F3/R9 interface in talin F2R9 (D1676R, E1770K, M319A) affects it’s ability to bind to MLVs as compared to wild type F2R9.
3. Weakening of the Talin F2F3/Talin R9 autoinhibitory interface leads to talin mediated integrin activation. We will use NMR to determine the chemical shift perturbation of labeled integrin β_3 cytoplasmic tail in presence of F2F3, F2R9 wild type , F2R9 mutant (D1676R, M319A, E1770K) and FL talin. We will also determine the integrin $\alpha_{IIb}\beta_3$ activation caused by talin FL and talin FL mutant (T1767L, E177K, M319A) in CHO cells. The talin FL mutant (T1767L, E1770K, M319A) bears three mutations in it’s F2F3/R9 autoinhibitory interface which help to weaken the autoinhbitory interaction in talin.
4. Investigate the reported actin binding sites in talin and examine how they may also be autoinhibited in full length talin. We will use purified talin fragments F2F3, R1-R9, R13, R13-DD, F2R9, F2R10, F2R12, F2DD, FL and FL mutant

(T1767L, E1770K, M319A) in the F-actin cosedimentation assay to determine the actin binding sites in talin and to compare the ability of different talin fragments to bind to F-actin.

CHAPTER II

MATERIALS AND METHODS

2.1 Protein Preparation and Purification

Talin fragments F2R9 (206-1848), F2R10 (206-1973), F2R12 (206-2294), F2DD (206-2541), R1R9 (486-1848) and F0DD (1-2541) (figure 2) were subcloned into the parallel His-1 vector pET 28t containing a N-terminal His- tag. The talin fragments were expressed in *E.coli* strain BL21 (DE3) and the cells were lysed using 10 mg/ml lysozyme. All the talin fragments were purified on nickel affinity column as described previously (Begona et al., 2003). Briefly, the proteins were eluted with 250mM imidazole in the elution buffer (20mM Tris-HCl, 500mM NaCl, 1mM DTT, pH 8.0). The eluted proteins were dialyzed against the dialysis buffer (20mM Tris-HCl, 150mM NaCl, 1mM DTT, pH7.4). The proteins were further purified by size exclusion chromatography. Superdex-200 (Amersham Biosciences) was used for F2R9, F2R10 and F2R12 and Superose-6 was used for other talin fragments. Talin F2F3 (206-405) and R9 (1654-1848) were prepared as described previously (Goksoy et al., 2008). Triple mutation of talin F2R9 (D1676R,

E1770K, M319A) FL (H1711E, T1812E, N1815E) and FL(T1767L, M319A, E1770K) were made using QuickChange Site-Directed mutagenesis (Stratagene) and prepared in the same way as wild type.

2.2. Lipid Vesicle Preparation and Lipid Cosedimentation Assay

The phospholipids such as POPC, POPS, PIP2 (figure 8) used to make multilamellar vesicles (MLV) were purchased from Avanti Polar Lipids (Alabaster, AL, USA). The lipids were dissolved together in chloroform in a vial. The chloroform was removed under a stream of nitrogen followed by lyophilization. The lipids formed a film inside the vials. The lipid film was then hydrated in the phosphate buffer (50 mM Na_2HPO_4/NaH_2PO_4, 50 mM NaCl, 2mM NaN_3, and pH 6.8) followed by homogenization with repeated freeze thaw cycles to form MLVs. The MLVs were mixed with purified talin fragments F2F3 (206-405), F2R9 (206-1848), FL (1-2541), F2DD (206-2541), FL mutant (H1711E, T1812E, N1815E) and F2R9 mutant (D1676R, E1770K, M319A) in separate centrifuge tubes in molar ratio of 1:20 on a shaker at room temperature for 20 minutes followed by centrifugation at 14000 rpm for 30 minutes. The lipids formed a pellet at the bottom of the centrifuge tubes. The pellets were resuspended in 40 µl 1X SDS and 10µl of 4X SDS was added to supernatant from all the samples.

2.3 Actin Cosedimentation Assay

Actin purified from rabbit skeletal muscle was purchased from Cytoskeleton. Actin and purified talin fragments F2F3 (206-405), F2R9 (206-1848), F2R10 (206-1973), F2R12 (206-2294), F2DD (206-2541), FL (1-2541), R13-DD (2300-2541), R13 (2300-2482) and FL mutant (M319A, E1770K, T1767L) were mixed in separate centrifuge tubes in a molar ratio of 1:2 in a total volume of 50 µl of F-actin buffer (10mM tris-Hcl pH 8.0, 0.2mM ATP, 0.2 mM DTT, 0.2mM CaCl2 and 100 mM NaCl). The samples were then incubated at room temperature for 20 minutes and centrifuged at 63000 rpm at 24 C for 90 minutes. The supernatant was removed in separate tubes and pellets were washed carefully with F-actin buffer. The pellets were resuspended in 60 µl of 1X SDS. 10µl of 4X SDS was added to supernatant from all the samples. Equal volumes of pellet and supernatant were loaded onto 4-20% Tris-glycine gels and protein content of the samples was resolved by SDS-PAGE. The gels were stained by Coomassie blue and the intensity of bands on gel was analysed using Image J.

2.4 NMR Spectroscopy

The heteronuclear NMR experiments were performed at 25 °C on Bruker Avance 600 MHz spectrometers equipped with cryogenic triple resonance probes and shielded z-gradient units as described previously (Song et al, 2012). The HSQC experiments to determine the interaction between talin and integrin β_3 cytoplasmic tail (CT) were performed with ^{15}N-labeled β_3 CT and unlabeled talin F2F3, F2R9, F2R9 mutant

(D1676R, E1770K, M319A) and full length in phosphate buffer (50 mM Na_2HPO_4/NaH_2PO_4, 50 mM NaCl, 2mM NaN_3, and pH 6.8). The weighted chemical shift changes of amide proton and nitrogen were calculated using the equation: $\Delta\delta_{obs[HN,N]}=([\Delta\delta_{HN}W_{HN}]^2+[\Delta\delta_N W_N]^2)^{1/2}$, where W_{HN} (1.0) and W_N (0.154) are weighting factors based on the gyromagnetic ratios of ^1H and ^{15}N. NMR data was processed and analyzed using nmrPipe (Delaglio et al., 1995), PIPP (Garrett et al., 1991) and Sparky (Lee et al., 2009).

2.5 Integrin αιιbβ3 Activation Assay

Chinese hamster ovary (CHO) cells stably expressing integrin αιιbβ3 were transfected with EGFP vector alone, full length talin wild type and full length talin mutant (T1767L, M319A, E1770K). The effects of full length talin and and talin mutant on integrin were evaluated with PAC1, a monoclonal antibody which specifically recognizes active αιιbβ3 as described previously (Ma et al., 2008; Goksoy et al., 2008). Briefly, 24 hours after transfection, the cells were harvested and stained with PAC1 followed by Alexa Fluor 633 goat anti-mouse IgM conjugate. The cells were then washed, fixed and analyzed by Flow Cytometry, gating only on the EGFP positive cells. Mean Fluorescence intensities (MFI) of PAC1 bound to EGFP-talin or EGFP-talin mutant expressing cells were compared with MFI of PAC1 bound to the CHO cells expressing EGFP vector alone. Three independent experiments were performed, and the T-student test was used for statistical analysis.

CHAPTER III

RESULTS AND DISCUSSION

3.1 Results

3.1.1 PIP2 regulates membrane localization and activation of talin

Talin F2F3 contains stretch of positively charged residues which enables talin to bind membrane and mediate integrin activation by binding to cytoplasmic tails of integrin's β subunit (Kalli et al., 2013; Song et al., 2012). Also, Talin recruits PIPKIγ kinase which in turn enriches membrane with lipid phosphatidylinositol-4, 5-bisphosphate (PIP2) (Paolo et al., 2002). PIP2 helps to activate autoinhibited talin (Goksoy et al., 2008). The structure of talin F3-R9 autoinhibitory complex (Figure 5, 6), showed a stretch of negatively charged residues on talin R9 which is located on the same side as stretch of positively charged residues on F2F3 (Song et al., 2012).

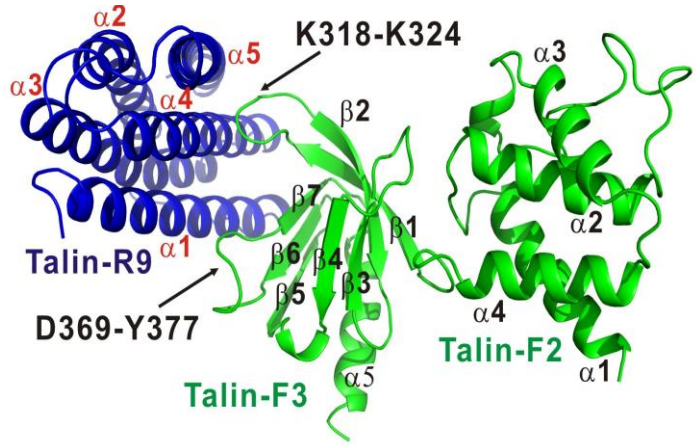

Figure 5 Crystal structure of talin-F2F3-R9 autoinhibitory complex. The talin head subdomains F2 and F2 are shown in green and talin rod subdomain R9 is shown in blue (adapted from Song et al ., 2012).

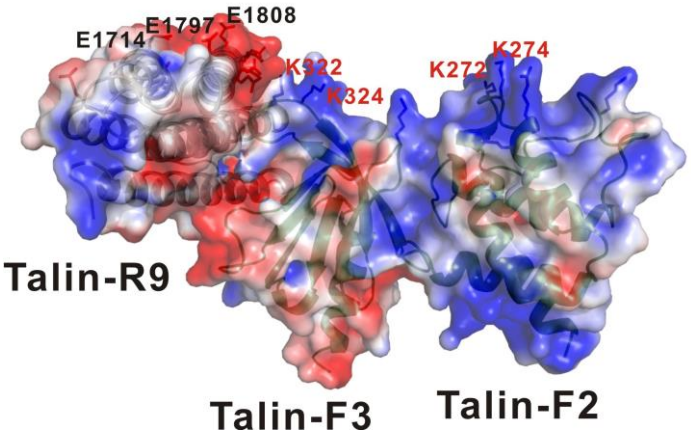

Figure 6 The positive charge enriched region is shown in blue and negative charge enriched region is shown in red. A stretch of positive charged residues on talin F2F3 is located on the same side as a stretch of negatively charged residues on talin R9 (adapted from Song et al., 2012)

We found that binding of free F2F3 to R9 was disrupted by addition of multilamellar vesicles (MLV) containing PIP2 to the F2F3-R9 complex using NMR based competition experiments. Also, PIP2 was shown to bind F2F3 bivalently.

In the present study, we used MLVs (multilamellar vesicles) in lipid cosedimentation assay to simulate the plasma membrane *in vitro*. We used the lipids PIP2, POPS and POPC to prepare the MLVS, all of which are found on the inner surface of plasma membrane (Figure 7-9).

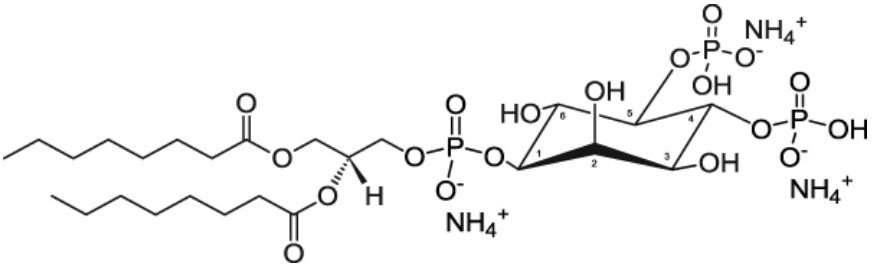

Figure 7 Chemical structure of PIP2(Phosphatidylinositol-4,5-bisphosphate)

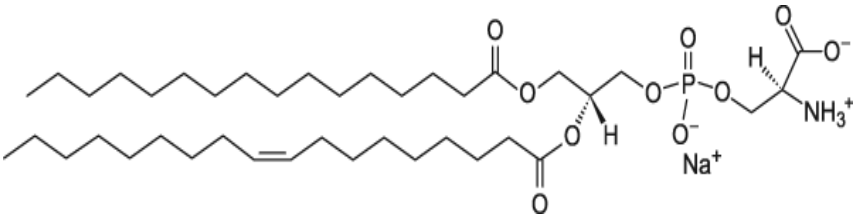

Figure 8 Chemical structure of POPS (palmitoyl-2-oleoyl-sn-glycero-3-[phosphor-L-serine])

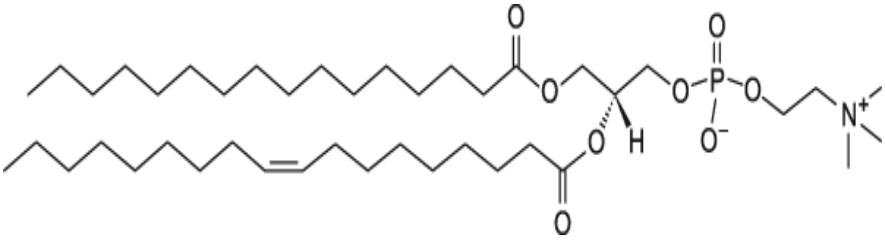

Figure 9 Chemical structure of POPC (1-palmitoyl-2-oleoyl-sn-glycero-3-phosphocholine)

For the lipid cosedimentation assay, we prepared MLVs containing only POPC as well as MLVs of mixed lipids (20% POPS; 80% POPC and 20% PIP2; 20% POPS, 60% POPC). To study the effect of negatively charged surface on rod domain of talin on the membrane binding ability of talin, we mixed together purified talin fragments F2F3,

F2DD, R1-R9, R9 and FL talin in separate centrifuge tubes along with MLVs. Upon centrifugation of all the samples at 13000 rpm at room temperature for 30 minutes, the MLVs formed a pellet at the bottom of the centrifuge tubes. We resolved the amount of protein present in the pellet and supernatant of all the samples by SDS-PAGE.

We found that F2F3 showed strong binding to membrane with most of it pelleting down along with the MLVs at 20% PIP2 (figure 10, 14). MLVs containing 20% PIP2 showed stronger binding to talin F2F3 as compared to MLVs containing 20% POPS and POPC due to the presence of higher negative charge on the head group (inositol-1,4,5-trisphosphate) of PIP2.

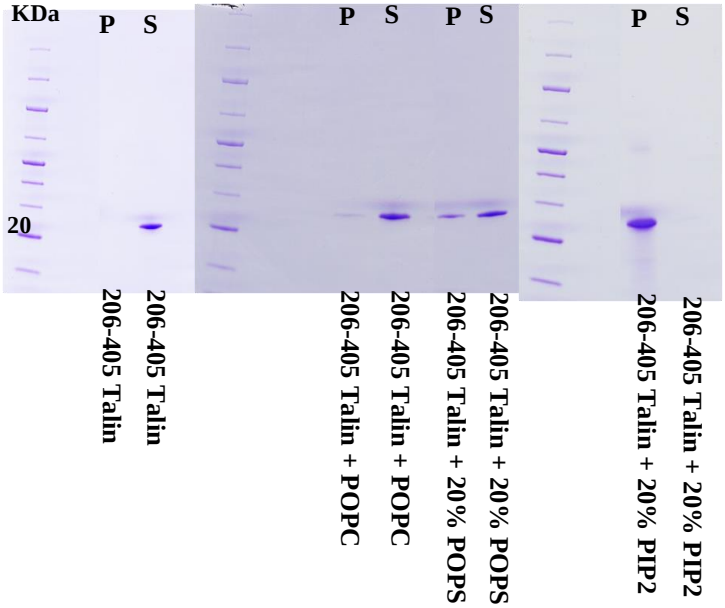

Figure 10 Lipid cosedimentation assay: In presence of MLVs enriched in 20% PIP2 whole of the talin F2F3 was found bound to MLVs in the pellet. Talin F2F3 shows significantly increased binding to MLVs containing 20 % PIP2 as compared to MLVs containing 20% POPS and POPC due to higher negative charge on head group of PIP2 as compared to POPS and POPC.

F2DD and FL talin showed lesser binding to membrane with most of the protein remaining in the supernatant at 20% PIP2 (Figure 11,13,14). R9 and R1-R9 showed no binding to membrane (Figure 12).

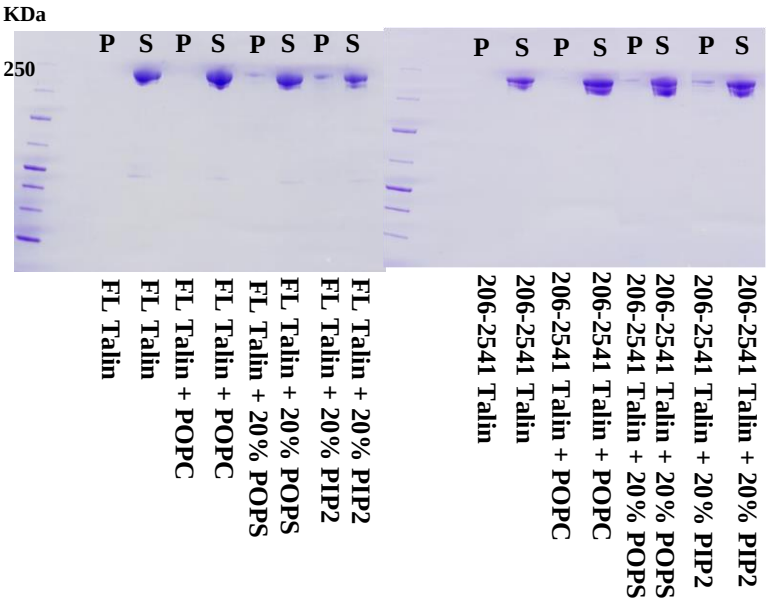

Figure 11 Lipid cosedimentation assay : Talin F2DD (206-2541) and FL(1-2541) did not pellet down in absence of MLVs. In presence of MLVs containing 20 % PIP2, talin F2DD and FL showed little binding to MLVs.

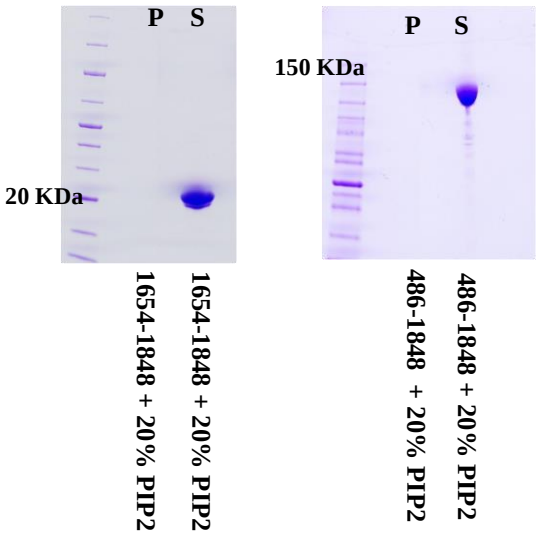

Figure 12 Lipid cosedimentation assay: Talin R1-R9 (486-1848) and R9 (1654-1848) showed no binding to MLVs containing 20% PIP2.

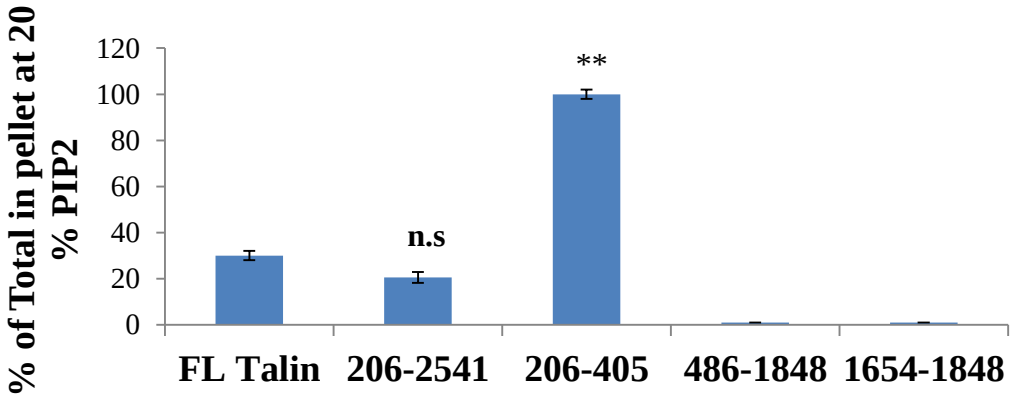

Figure 13 Image J was used to quantify the amount of protein in Figure 10, 11 and 12. The amount of talin is expressed as percent of total protein found in pellet. Bar graph represents mean ±S.E. (n≥3). N.S., not significant, p>0.05; *, p=0.01-0.05; **, p=0.001-0.01. Talin F2F3 (206-405) showed significantly higher binding to MLVs containing 20 % PIP2 as compared to F2DD (206-2541) and

FL talin (1-2541). Talin R1-R9 (486-1848) and R9 (1654-1848) showed no binding to MLVs containing 20% PIP2.

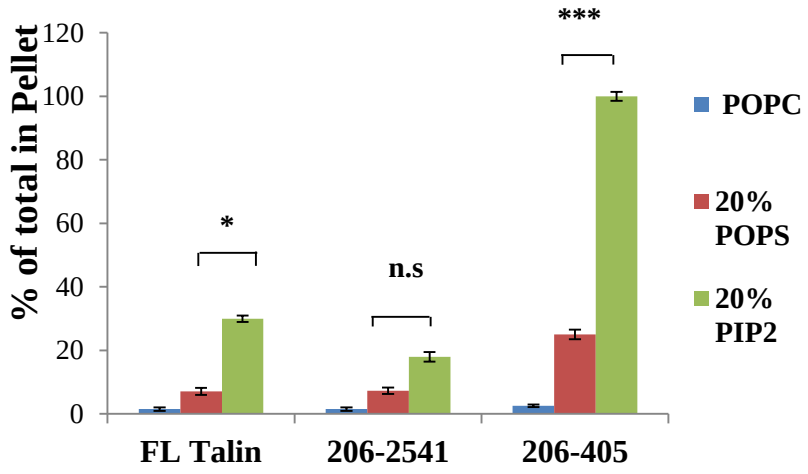

Figure 14 Image J was used to quantify the amount of protein in figure 10, 11. The amount of talin is expressed as percent of total protein found in pellet. Bar graph represents mean ±S.E. (n≥3). N.S., not significant, p>0.05; *, p=0.01-0.05; **, p=0.001-0.01;*, p<0.001. Talin F2F3 (206-405) and FL talin showed significantly higher binding to MLVs containing 20 % PIP2 as compared to MLVs containing 20% POPS.**

An increase in the concentration of NaCl in the buffer (20 mM Tris-HCl, 300mM NaCl, 1mM DTT, pH 8.0) used for the lipid cosedimentation assay resulted in impairment of electrostatic interaction between MLVs containing 20% PIP2 and the rod domain of talin and most of the talin F2R9 was found bound to the MLVs in pellet (figure 15).

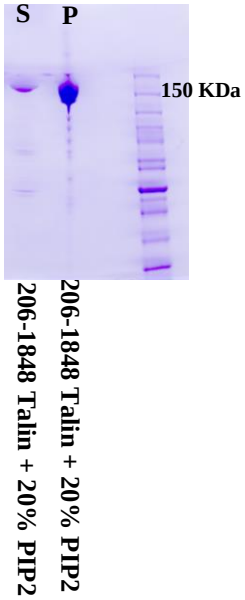

Figure 15 Lipid cosedimentation assay: Most of Talin F2R9 (206-1848) protein pelleted down along with MLVs containing 20% PIP2 due to an increase in the concentration of NaCl in buffer (20mM Tris-HCl, 300mM NaCL, 1mM DTT, pH 8.0) used for the assay. The higher concentration of NaCl impaired the electrostatic interaction between the MLVs and negatively charged R9.

We prepared MLVs enriched in varying concentrations of PIP2 and POPC and kept the concentration of POPS (20%) constant. We used these MLVs enriched with 1% PIP2, 5% PIP2, 10% PIP2, 20% PIP2 and 50% PIP2 to find out whether gradual increase in concentration of PIP2 would increase the amount of talin bound to membrane. As shown in Figure 16, 17, talin F2F3 showed gradual increase in amount of protein cosedimenting with MLVs in pellet with increase in concentration of PIP2 in MLVs and whole of F2F3 was found in pellet at 20% PIP2.

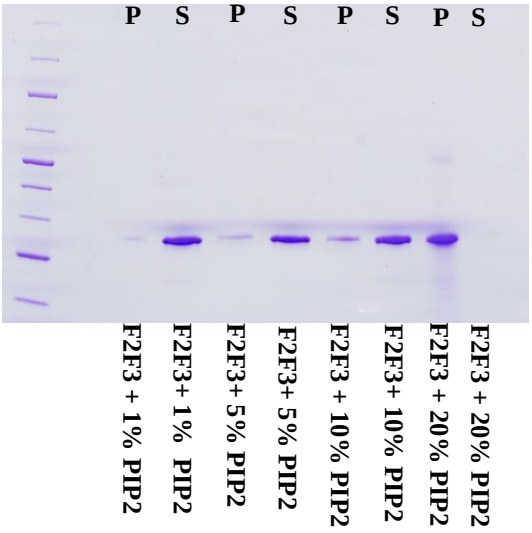

Figure 16 Lipid cosedimentation assay: The amount of Talin F2F3 (206-405) pelleting down with MLVs gradually increased with increase in the percentage of PIP2 (1-20%) in MLVs.

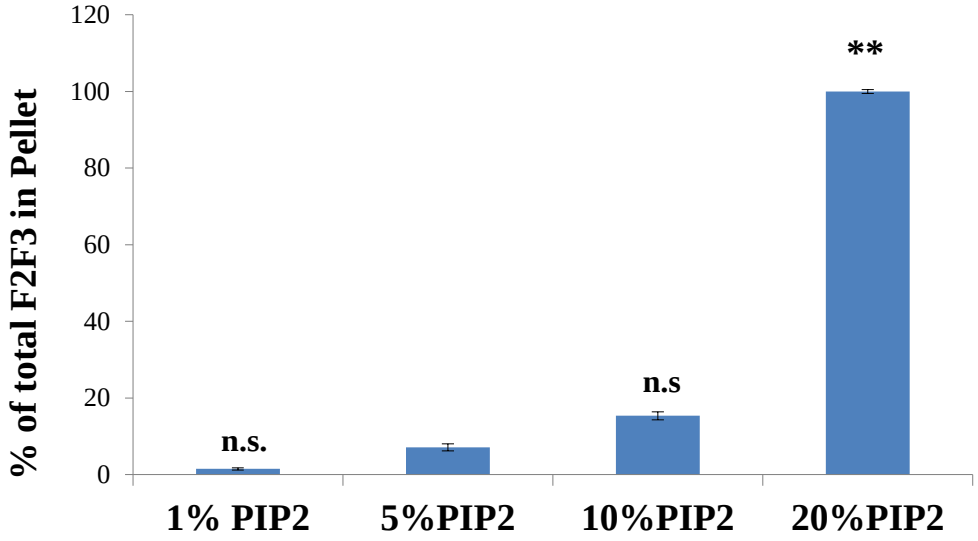

Figure 17 Image J was used to quantify the amount of protein in Figure 16. The amount of talin is expressed as percent of total protein found in pellet. Bar graph represents mean ±S.E. (n≥3). N.S., not significant, p>0.05; ***, p<0.001. Talin F2F3 (206-405) shows strong binding to MLVs enriched in 20% PIP2.

At 50% PIP2 more than half of the total FL wild type talin was found in pellet (Figure 18, 19). In order to further increase the repulsion between R9 and membrane we mutated three residues in the R9 domain to make talin 3E mutant (H1711E, T1812E, N1815E). As shown in figure 18, 19, at 20% PIP2 almost whole of the 3E mutant was in the supernatant and at 50% PIP2 the amount of 3E mutant which pelleted down was significantly less as compared to wild type FL talin. These findings suggest that the electrostatic repulsion between the negatively charged surface on R9 and membrane prevents membrane localization of autoinhibited talin.

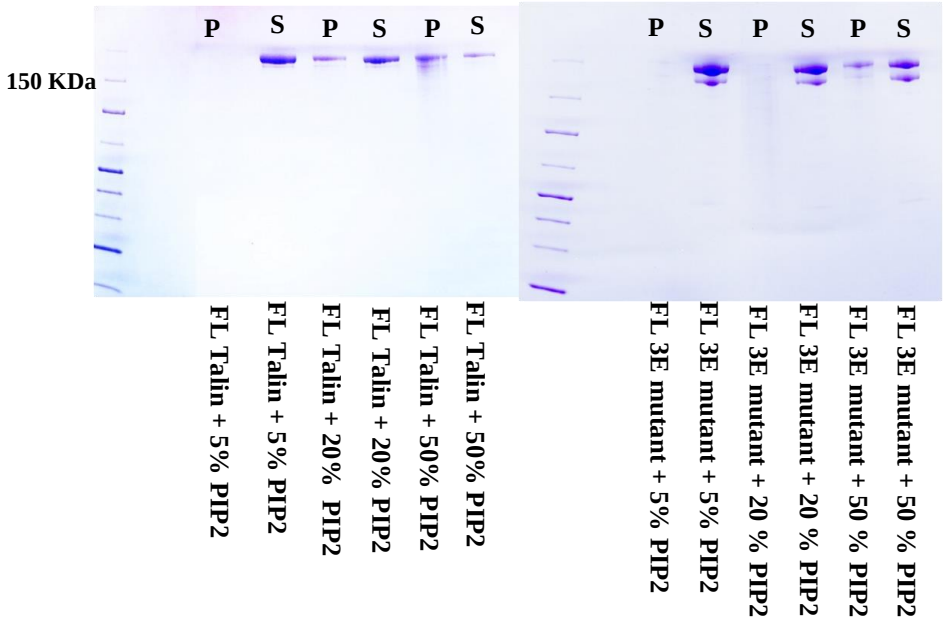

Figure 18 Lipid cosedimentation assay: The amount of wild type FL talin which pellets down with MLVs gradually increases with increase in percentage of PIP2 in MLVs. At 50% PIP2 approximately 60% of total FL talin goes to pellet along with MLVs. FL 3E mutant (H1711E, T1812E, N1815E) shows significantly reduced binding to MLVs containing 20% PIP2 and 50% PIP2 as compared to wild type FL talin. The increased repulsion between the rod domain of talin 3E mutant and MLVs containing 20% PIP2 and 50% PIP2 results in reduced binding of FL 3E mutant to MLVs.

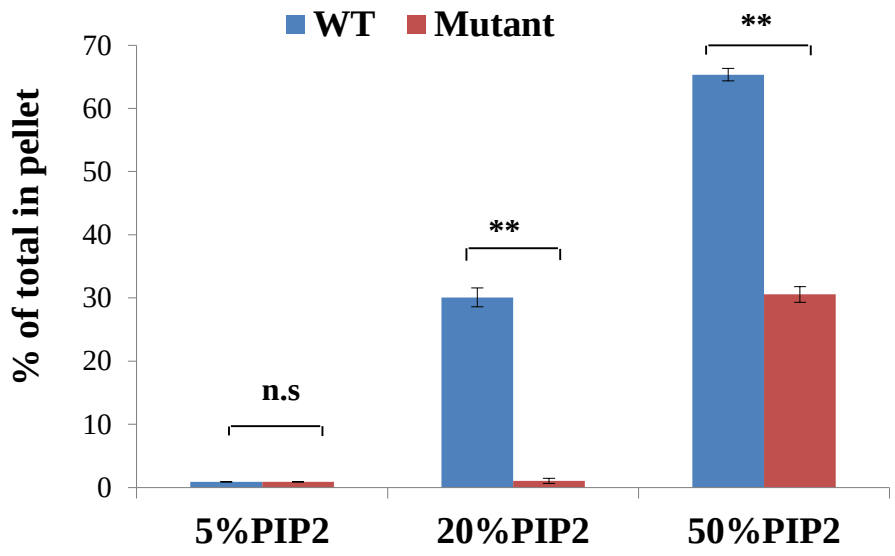

Figure 19 Image J was used to quantify the amount of protein in figure 18. The amount of talin is expressed as percent of total protein found in pellet. Bar graph represents mean ±S.E. (n≥3). N.S., not significant, **, p=0.001-0.01. Talin 3E mutant (H1711E, T1812E, N1815E) showed significantly reduced binding to MLVs containing 20% PIP2 and 50% PIP2 as compared to wild type FL talin.

Next we wanted to test the hypothesis that enrichment of membrane with negatively charged phospholipid PIP2 strongly attracts positively charged surface on talin-H and simultaneously repels negatively charged talin R9 and therefore promotes membrane localization and activation of autoinhibited talin. Based on the crystal structure of F2F3/R9 autoinhibitory complex (figure 20-21), we made a talin F2R9 (206-1848) triple mutant (D1676 R, E1770K, M319A) to weaken the autoinhibitory interaction of talin F2F3 and R9.

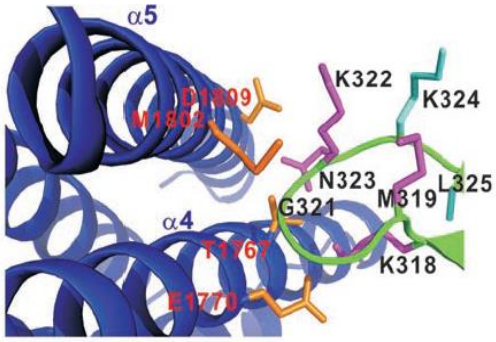

Figure 20 Close-up view of talin F2F3/ R9 interface shows the amino acid side chains of residues (K318-K324) (adapted from Song et al., 2012).

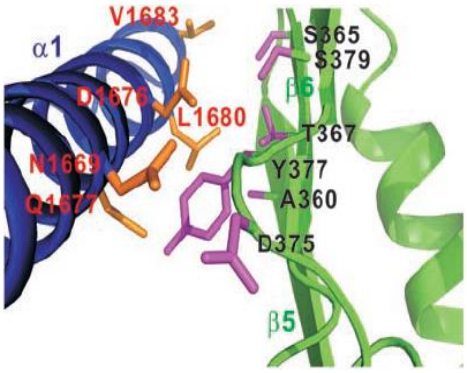

Figure 21 Close-up view of talin F2F3/ R9 interface shows the amino acid side chains of residues (D369-Y377) (adapted from Song et al., 2012).

The F2R9 triple mutant showed an increased binding to membrane even at 5% PIP2 as compared to wild type F2R9 (Figure 22, 23). At 50% PIP2, the F2R9 active mutant completely cosedimented with MLVs in pellet.

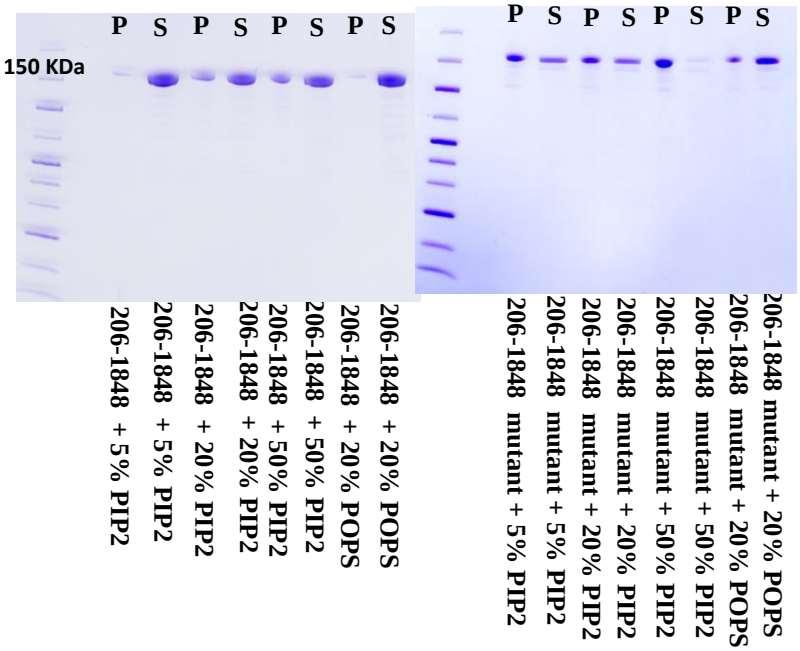

Figure 22 Lipid cosedimentation assay: Approximately 35% of total Talin F2R9 (206-1848) wild type pellets down with MLVs containing 20% PIP2 and 50% PIP2 due to pulling of positively charged F2F3 towards MLVs and pushing away of negatively charged R9 from MLVs. Weakening of the autoinhibitory interface in F2R9 (206-1848) mutant (D1676R, E1770K, M319A) causes significantly increased binding of the F2R9 mutant to MLVs lower percentage (5%) of PIP2 as well as at higher (50%) of PIP2 as compared to wild type F2R9.

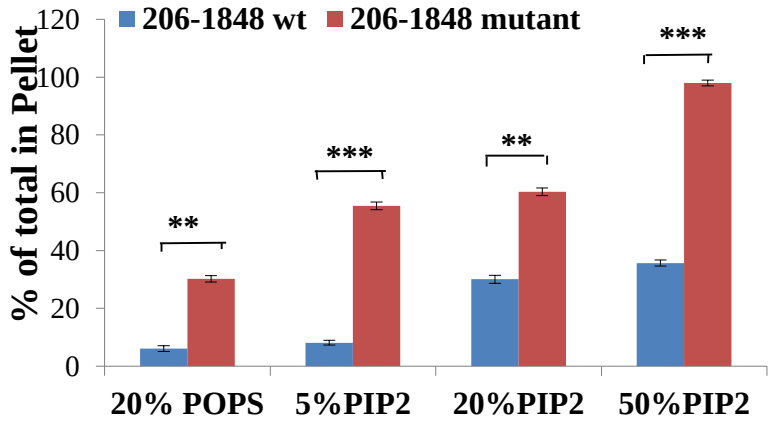

Figure 23 Image J was used to quantify the amount of protein in figure 22. The amount of talin is expressed as percent of total protein found in pellet. Bar graph represents mean ±S.E. (n≥3). N.S.,

not significant, p>0.05; **, p=0.001-0.01;*, p<0.001. Due to weakening of the F2F3/R9 autoinhibitory interface, talin F2R9 (206-1848) mutant (D1676R, E1770K, M319A) showed significantly increased binding to MLVs containing 20%POPS, 5%PIP2, 20% PIP2 and 50% PIP2 as compared to wild type F2R9.**

The above findings suggest that electrostatic repulsion between negatively charged membrane (MLVs) and the rod domain of talin significantly reduced the amount of FL and F2DD talin which bound to MLVs enriched in 20% PIP2. On the other hand whole of talin F2F3 could bind to the pellet containing MLVs enriched in 20% PIP2 due to the absence of negatively charged talin rod domain. An increase in the percentage of PIP2 in MLVs to 50% led to strong pulling of the positively charged talin F2F3 towards membrane and pushing of R9 away from the membrane which in turn resulted in increased amount of FL talin pelleting down along with MLVs. Due to further increase in repulsion between the rod domain of FL 3E mutant (H1711E, T1812E, N1815E) and MLVs, the amount of FL 3E mutant which bound to MLVs at 20% PIP2 and 50% PIP2 was significantly reduced as compared to wild type FL talin. The weakening of talinF3/R9 autoinhibitory interaction in F2R9 mutant (D1676R, E1770K, E1770K) promoted the pulling of F2F3 towards membrane and pushing away of R9 away from the the membrane. Therefore, F2R9 mutant (D1676R, E1770K, E1770K) showed significantly enhanced binding to membrane as compared to wild type F2R9. This finding supports the hypothesis that enrichment of membrane with PIP2 promotes membrane localization and activation of talin via a “pull-push” mechanism.

3.1.2 Disruption of F2F3-R9 autoinhibitory interface of talin leads to integrin activation

Extensive cell based, genetic and biochemical studies have shown that talin is required for integrin activation. In our previous studies, we have shown that talin R9 self-masks the integrin binding site in F3 domain and competes with integrin β-MP-CT for binding to it (Goksoy et al., 2008). This implies that disruption of Talin F2F3-R9 interface is required for activation of cytosolic talin in cells. We used 2D ^{1}H -^{15}N HSQC (heteronuclear single quantum correlation) to study the interaction between ^{15}N-labeled integrin β_3 cytoplasmic tail and unlabeled Talin F2F3, wild type Talin F2R9 and F2R9 triple mutant (D1676R, E1770K, M319A) and FL talin (Figure 24). All the proteins were well folded as determined by its chemical shift dispersion pattern. We found that F2R9 wild type had little effect on the HSQC spectrum of integrin β_3 CT as compared to talin F2F3 which caused chemical shift perturbation in the membrane proximal region of β_3 CT. F2R9 wt showed some perturbation particularly in the membrane distal region of integrin. On the other hand the triple mutant of F2R9 showed enhanced binding to β_3 CT as compared to F2R9 wild type and caused perturbation in the membrane proximal region of integrin-β_3 CT.

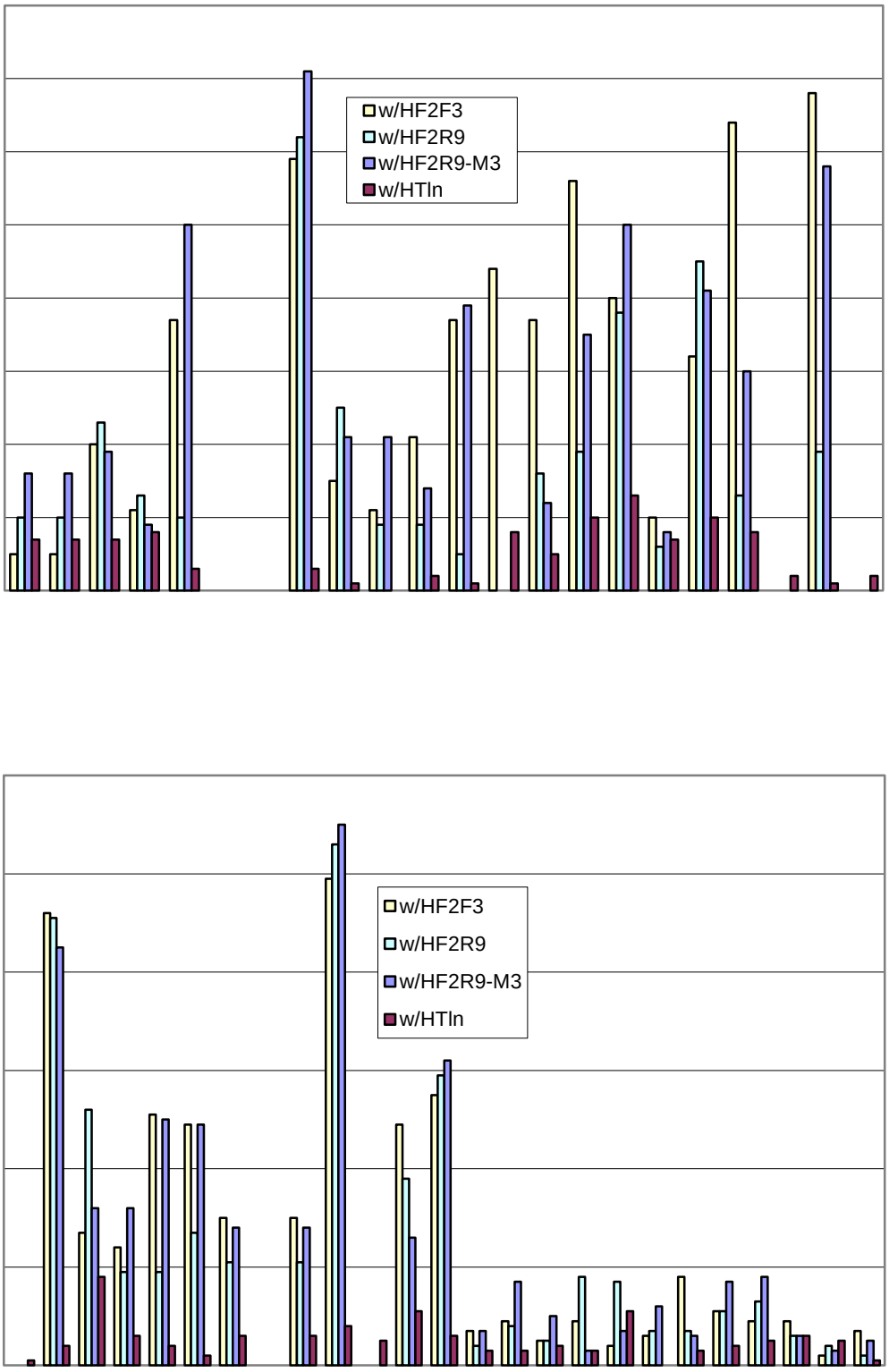

Figure 24 Chemical shift perturbation profiles for integrin β_3 CT upon binding to Talin F2F3, F2R9, F2R9 (M319A E1770K T1767L) and FL talin (Tln). The residues in membrane proximal region of

integrin β_3 CT were significantly perturbed by Talin F2F3 and F2R9 mutant (T1767L M319A E1770K). F2R9 caused some chemical shift changes in membrane distal region. (Residues whose signals were diminished due to severe line- broadening are indicated by *)

We transfected Chinese hamster ovary (CHO) cell line stably expressing integrin $\alpha IIb\beta_3$ with FL talin wild type and FL talin triple mutant (M319A, E1770K, T1767L) EGFP constructs. We used a mAb (PAC1) which specifically recognizes activated $\alpha IIb\beta_3$ integrin to determine the activation state of $\alpha IIb\beta_3$ in these cells by FACS. The data in figure 25 from three independent experiments shows that the FL talin triple mutant could bind and activate $\alpha IIb\beta_3$ integrin significantly better than FL talin wild type in CHO cells. These results are consistent with those obtained from HSQC experiments (figure 24).

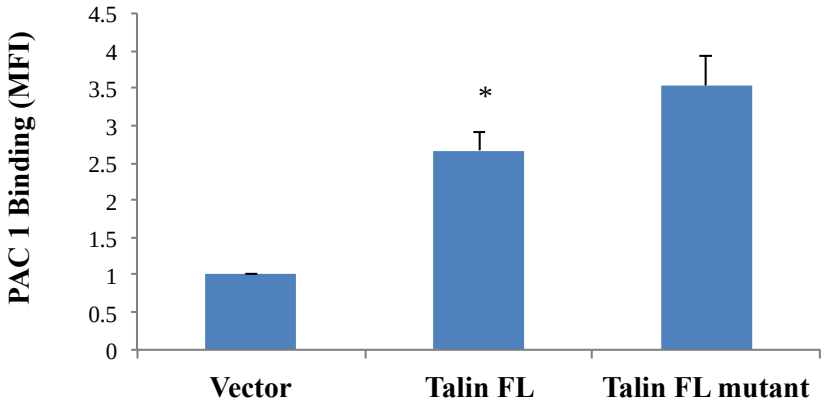

Figure 25 Comparison of the activation of integrin $\alpha_{IIb}\beta_3$ by Full length (FL) wild type talin and FL talin mutant (T1767L M319A E1770K). As described previously (Ma et al., 2008), the effects of FL wild type talin and talin mutant (T1767L M319A E1770K) on integrin activation were analyzed using CHO cells stably expressing integrin $\alpha_{IIb}\beta_3$ and an activation specific mAb (PAC 1). The weakening of the F2F3/R9 autoinhibitory interface in FL talin mutant (T1767L M319A E1770K) significantly enhanced it's ability to activate integrin $\alpha_{IIb}\beta_3$ in CHO cells as compared to wild type FL talin. The data are representative of three independent experiments (means±SE). ($n \geq 3$) $p>0.05$; * indicates $p<0.05$.

3.1.3 FL Talin is Conformationaly Restricted to Bind Actin

Talin is known to act as a linker between integrins and actin cytoskeleton. Talin has been suggested to contain atleast three actin binding sites. It has been shown to be able to bind both G-actin and F-actin in cosedimentation assay (Muguruma et al., 1990). In the presence of MgCl2 and KCl, Talin stimulates the rate of polymerization of G-actin. However, Talin has not been shown to affect final viscosity of F-actin and was therefore suggested to lack the ability to cross-link or bundle actin filaments.

In the present study we used talin F2F3 (206-405), F2R9 (206-1848), F2R10 (206-1973), F2R12 (206-2294), F2DD (206-2541), FL, R13DD (2300-2541), R13 (2300-2482) and R9 (1654-1848) to investigate the reported actin binding sites in talin. The monomeric form of actin (Globular actin) and purified talin fragments were mixed together in separate centrifuge tubes in a molar ratio of 1:2 in F-actin buffer (10mM tris-Hcl pH 8.0, 0.2mM ATP, 0.2 mM DTT, 0.2mM CaCl2 and 100 mM NaCl) which allowed G-actin to polymerize in to F-actin. The samples were then centrifuged at 63000 rpm at 24°C to separate F-actin from G-actin by differential sedimentation. The F-actin formed a pellet at the bottom of the centrifuge tubes.

We found that talin fragments F2F3, R1-R9 and R13-DD cosedimented with F-actin in pellet (Figure 26). This finding indicates the presence of an actin binding site on talin

F2F3, R1-R9 as well as R13-DD. Consistent with previous studies, Talin R13 (2300-2482) showed no binding to F-actin which indicates that DD (2494-2541)

contributes to the F- actin binding site on R13-DD (Gingras et al., 2008). Talin F2R9, F2R10 and F2R12 showed significantly enhanced binding to F-actin as compared to F2F3, R1-R9, FL, R13-DD and F2DD (figure 26, 27). This finding suggests that FL talin is conformationaly restricted to bind to F-actin.

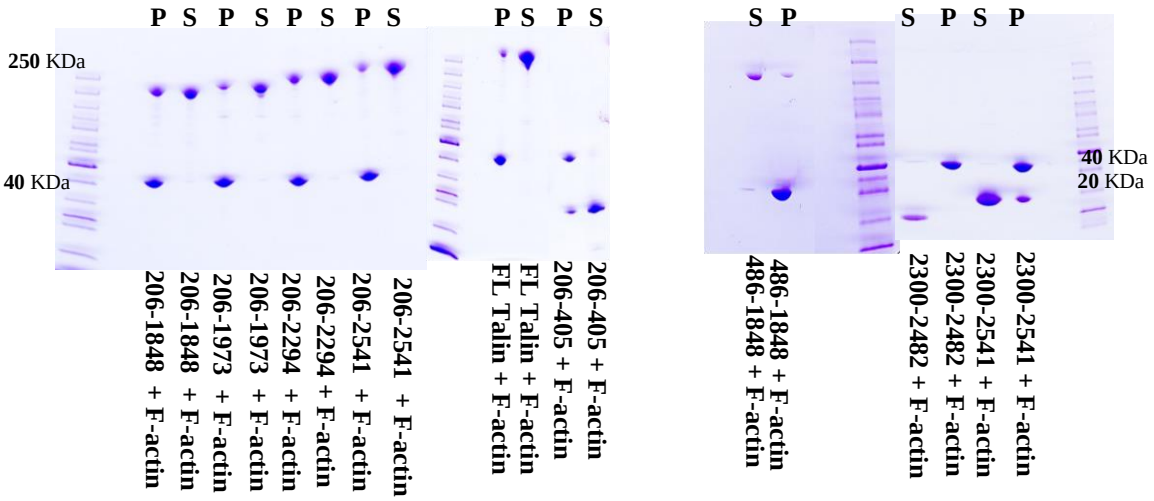

Figure 26 F-actin cosedimentation assay: F-actin (43 KDa) pelleted down at the bottom of the tubes following centrifugation at 63000 rpm at 24°C for 90 minutes. Talin F2F3, Talin R1-R9 (486-1848) and R13-DD (2300-2541) showed binding to F-actin in pellet which indicates the presence of an F-actin binding site on these talin fragments. Talin F2R9 (206-1848), F2R10 (206-1973) and F2R12 (206-2294) showed significantly enhanced binding to F-actin in pellet as compared to Talin F2F3 and R1-R9 which indicates the presence of an additional F-actin-binding site on the rod domain of talin. However, Talin F2DD and FL showed significantly reduced binding to F-actin as compared to F2R9, F2R10 and F2R12 which suggests that FL talin and F2DD are conformationaly restricted to bind to F-actin. R13 (2300-2482) showed no binding to F-actin suggesting that DD (2494-2541) contributes to the F-actin binding site on R13-DD (2300-2541)

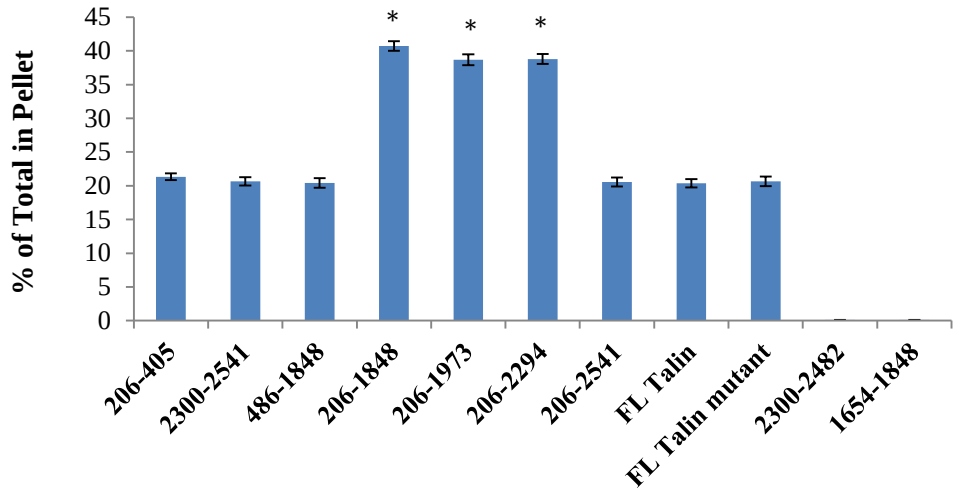

Figure 27 Image J was used to quantify the amount of protein in figure 26 and 28. The amount of talin is expressed as percent of total protein found in pellet. Bar graph represents mean ±S.E. (n≥3; *, p=0.01-0.05. Talin contains an actin binding site on F2F3 (206-405), R1-R9 (486-1848) and R13-DD (2300-2541). Talin F2R9 (206-1848), F2R10 (206-1973) and F2R12 (206-2294) showed significantly enhanced binding to F-actin as compared to talin F2F3, R1-R9, R13-DD, F2DD and FL talin. Talin FL and FL mutant (M319A, E1770K, T1767L) showed little binding to F-actin indicating that both the proteins are conformationaly restricted to bind to F-actin. Thus weakening of autoinhibitory F2F3/R9 interaction could not improve FL talin mutant's ability to bind to F-actin. R9 (1654-1848) and R13 (2300-2482) showed no binding to F-actin.

We compared the ability of FL active mutant (M319A, E1770K, T1767L) to bind to F-actin with that of wild type FL talin (figure 27, 28). The FL active mutant also showed little binding to F-actin similar to wild type FL talin. Thus weakening of the F3/R9 autoinbitory interaction in FL active mutant could not improve it's ability to bind to F-actin. The purified talin fragments dissolved in F-actin buffer did not pellet down at the bottom of the centrifuge tubes in absence of F-actin (figure 29).

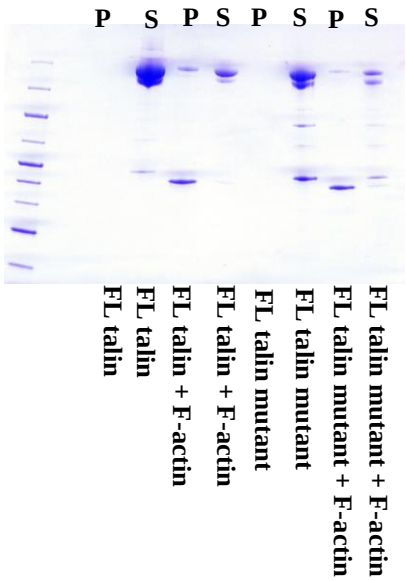

Figure 28 F-actin cosedimentation assay: FL talin and FL talin active mutant (M319A, E1770K, T1767L) proteins dissolved in F-actin buffer did not pellet down in absence of with F-actin (43 KDa). In presence of F-actin, both FL talin and FL talin active mutant (M319A, E1770K, T1767L) showed little binding to F-actin. Thus weakening of F2F3/ R9 autoinhibitory interface in FL talin active mutant did not improve it's ability to bind to F-actin.

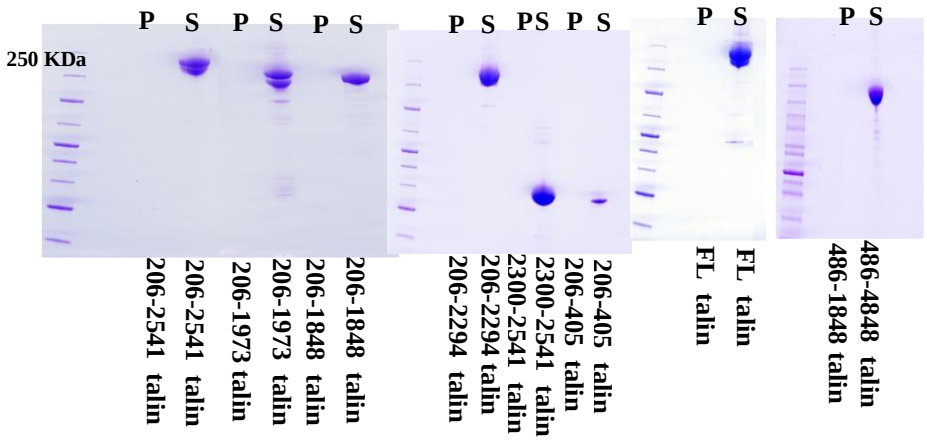

Figure 29: The purified talin fragments F2F3 (206-405), F2R9 (206-1848), F2R10 (206-1973), F2R12 (206-2294), F2DD (206-2541), FL (1-2541), R1-R9 (486-1848), R13DD (2300-2541) and FL talin were dissolved in F-actin buffer. The purified talin fragments did not pellet down following centrifugation at 63000 rpm at 24°C for 90 minutes in absence of F-actin.

The above findings show that FL talin contains an actin binding site on F2F3, R1-R9 and R13-DD. An additive effect of the actin binding sites on F2F3 and R1-R9 could lead to the enhanced binding of talin F2R9, F2R10 and F2R12 to F-actin. However, significantly reduced binding of FL talin to F-actin as compared to F2R9, F2R10 and F2R12 suggests that FL talin is conformationaly restricted to bind to F-actin. The little binding of FL talin to F-actin could be due to the masking of any of the actin binding sites in FL talin by R13-DD. The FL talin active mutant (M319A, E1770K, T1767L) which showed enhanced binding to integrin did not show enhanced binding to F-actin. This finding suggests that the two binding events are regulated by different conformational activation mechanisms.

3.2 Discussion

Integrin mediated cell adhesion and their ability to couple extracellular matrix to actin cytoskeleton is vital to physiological and pathological processes such as platelet adhesion, leukocyte transmigration, tumor vascularization and metastasis (Hynes et al., 2002; Brooks et al., 1994; Berlin et al.,1995). Talin is an adaptor protein which plays an important role in the function of integrins by regulating activation of integrins and linking integrins to actin (Luo et al., 2007; Qin J. et al., 2004). The integrin binding site in Talin F2F3 domain is self-masked by R9 (Figure 2,5) such that talin is autoinhibited to bind integrin β cytoplasmic tail (Goksoy et al., 2008; Song et al.; 2012).

Talin is randomly distributed in cytoplasm in inactivated platelets and fibroblasts. Upon stimulation of these cells by an agonist talin has been shown to be localised to membrane (Beckerle et al., 1989; Banno et al., 2012). PIP2 has been shown to activate talin (Goksoy et al., 2008). The results from our lipid co-sedimentation assay show that talin F2F3 binds MLVs containing 20% PIP2 strongly as compared to talin FL and F2DD (Figure 10-14). The structure of F3-R9 autoinhibitory complex revealed a stretch of negatively charged residues on R9 which is located on the same side as the stretch of positively charged residues on F2F3 (figure 6; Song et al.,2012). In lipid cosedimentation assays, FL wild type talin showed enhanced binding to MLVs enriched with higher concentration of PIP2 (50%) as compared to MLVs containing lower concentration of

PIP2 (Figure 18). Also, the full length talin mutant (talin-3E mutant) showed significantly reduced binding to MLVs containing higher concentration of PIP2 (50%) as compared to wild type full length talin (figure 18,19). These findings support the hypothesis that electrostatic repulsion between the negatively charged talin-R9 and membrane promotes cytosolic retention of autoinhibited talin.

The active mutant of talin F2R9 (D1676R, E1770K, M319A) shows stronger binding to membrane as compared to the wild type talin F2R9 (Figure 22,23). Thus weakening of the talin F3/R9 autoinhibition substantially enhances the binding of talin to membrane by promoting the "pulling" of positively charged surface on talin-H to membrane and " pushing" away of negatively charged surface on talin-R from membrane. This finding supports the hypothesis that enrichment of membrane with negatively charged PIP2 promotes membrane localization and activation of autoinhibited talin via a "pull-push". mechanism. However, approximately 60% of the total FL wild type talin pellets down with MLVs enriched with higher percentage (50%) of PIP2 (figure 18,19) which suggests the involvement of other cellular mechanisms in regulating activation of talin and its localization from cytosol to membrane. Banno et al. (2012) have shown that an interdomain interaction between Talin 466-787, a region of talin containing two vinculin binding sites, and Talin F2F3 prevents localization of talin to membrane. RIAM (Rap1-GTP interacting adaptor molecule) which binds to both a member of Ras subfamily, Rap1 and talin has been shown to be required for activation of integrin $\alpha IIb\beta_3$ in CHO cells (Lee et al, 2009). Further investigation of the role of Rap1/RIAM in talin's localization to membrane and possibly it's activation would be helpful in understanding the mechanism

of talin mediated integrin activation. Also, the crystal structure of FL talin would be valuable in understanding how binding to membrane and integrin is inhibited in FL talin.

Active mutant of F2R9 (D1676R, E1770K, M319A) showed increased binding to integrin β_3 CT as compared to wild type talin F2R9 in NMR studies (Figure 24). Also FL active triple mutant (T1767L, E1770K, M319A) showed increased integrin activation in CHO cells (Figure 25). These results suggest that weakening of autoinhibition in talin enhances talin mediated integrin activation and also the ability of talin to bind to membrane. Perhaps localization of talin to membrane facilitates the interaction of talin with integrin. In our NMR studies, Talin F2F3 showed significant perturbation of integrin β_3 CT mainly in the membrane proximal region (figure 24). FL talin showed negligible binding to β_3 CT. F2R9 showed weak interaction with β_3 CT and caused some perturbation particularly in the membrane distal region of integrin β_3 CT (figure 24). This finding suggests that an additional fragment of talin rod domain is involved in inhibiting the interaction of FL talin with integrin.

Along with other proteins such as vinculin, talin forms a connection between extracellular matix and actin cytoskeleton at sites of adhesion to substrate in activated platelets and fibroblasts. The activation of these cells leads to redistribution talin to membrane and polymerization of actin filaments and change in shape of cell (Beckerle et al., 1989). Previous studies have indicated the presence actin binding sites on COOH terminus, head domain and in rod domain (Hemmings et al., 1996). We used actin cosedimentation assay in order to investigate the reported actin binding sites in talin. The monomeric form of actin, Globular actin (G-actin) has been shown polymerize to filamentous actin (F-actin) in physiological conditions such as 2mM $MgCl_2$ and 100 mM

KCl in presence of talin in invitro studies (Muguruma et al., 1990). Our study suggests the presence of an actin binding site on F2F3, R1-R9 and R13-DD domain of talin, each of which binds to F-actin (Figure 26). However, FL talin does not show additive binding to F-actin due to the presence of three actin binding sites (figure 27). It rather shows significantly reduced binding to F-actin as compared to F2R9, F2R10 and F2R12 which suggests that the FL talin is not only conformationaly restricted to bind integrin but also F-actin. The triple talin FL mutant (T1767L, E1770K M319A) also showed little binding to F-actin (figure 27, 28). Thus the disruption of the autoinhibitory F3/R9 interface in talin which masks the integrin binding site on F3 increased the binding of talin to integrin but not to actin. These findings suggest that binding of talin to integrin and actin is regulated by different conformational activation mechanisms. Further investigation of the mechanisms which regulate binding of talin to actin will help us better understand the role of talin in actin mediated changes in cell morphology and motility and focal adhesion turnover.

In summary, we have defined a “pull-push” mechanism which promotes membrane localization and activation of autoinhibited talin. Our results suggest that autoinhibited talin remains in cytosol due to electrostatic repulsion between negatively charged surface on R9 and plasma membrane. The enrichment of membrane with PIP2 promotes the pulling of positively charged talin-H to membrane and pushing away of negatively charged talin-R from membrane which in turn leads to localization of talin to membrane and it’s activation. Consistent with previous studies our results suggest the presence of three actin binding sites on talin. We found that full length talin adopts a conformation which not only prevents the integrin binding but also the binding of talin to actin. Our

studies suggest that the two binding events are regulated by different conformational activation mechanisms.

3.3 Elution Profiles of Proteins

Talin 206-1848 wild type

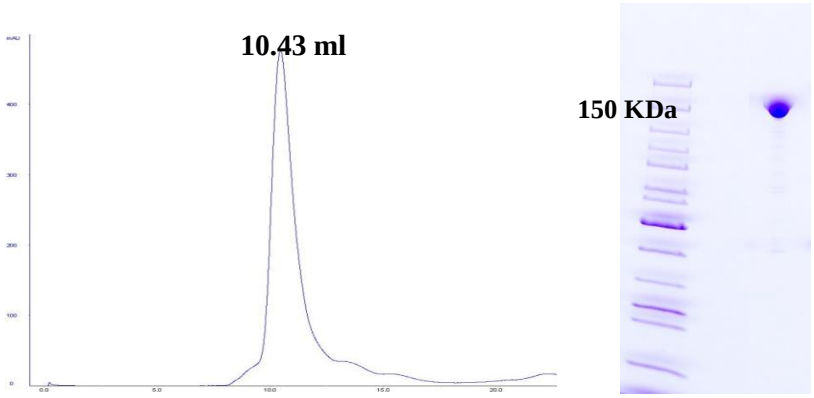

Superdex 200

Talin 206-1848 D1676R, E1770K, M319A

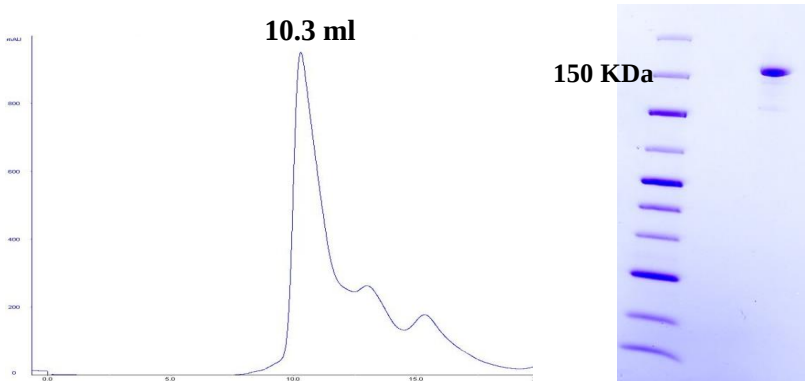

Superdex 200

Talin 206-1973

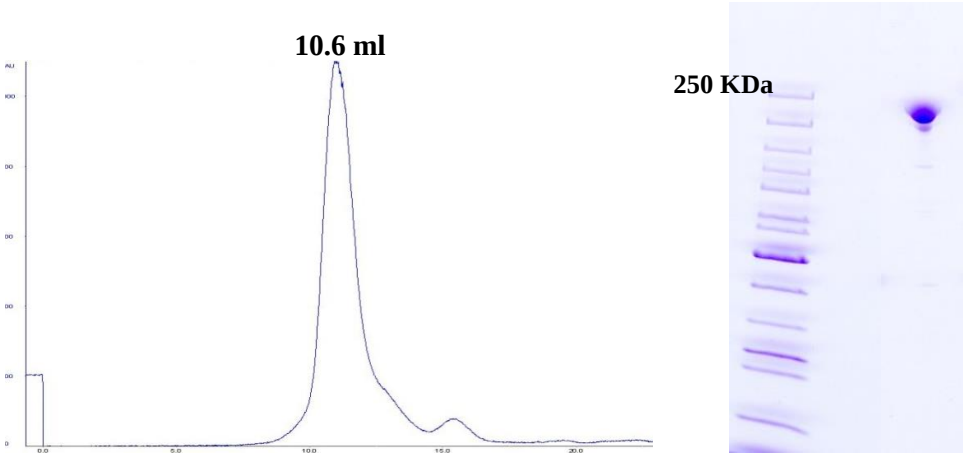

Superdex 200

Talin 206-2294

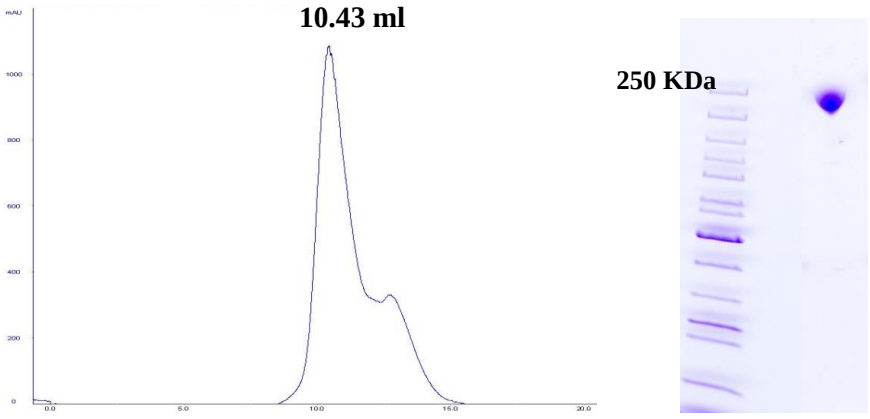

Superdex 200

Talin 206-2541

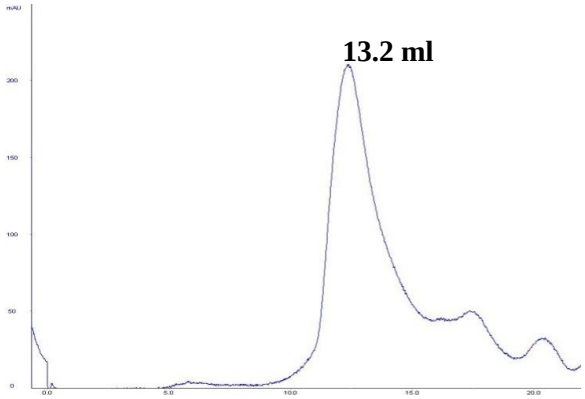

13.2 ml

250 KDa

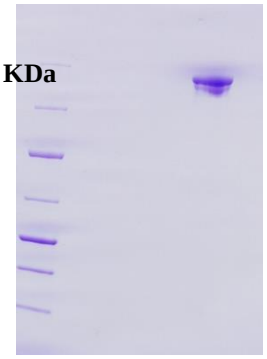

Superose 6

Talin full length (1-2541)

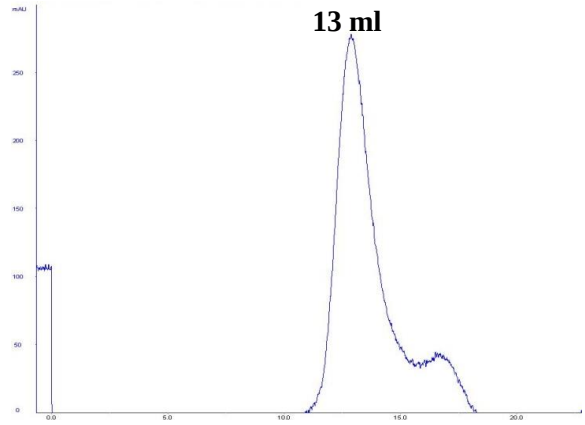

13 ml

250 KDa

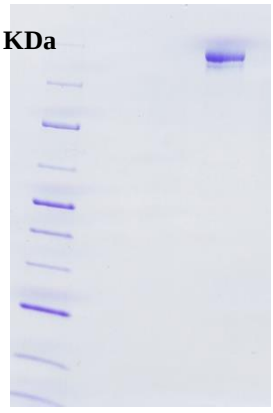

Superose 6

Talin full length H1711E, T1812E, N1815E

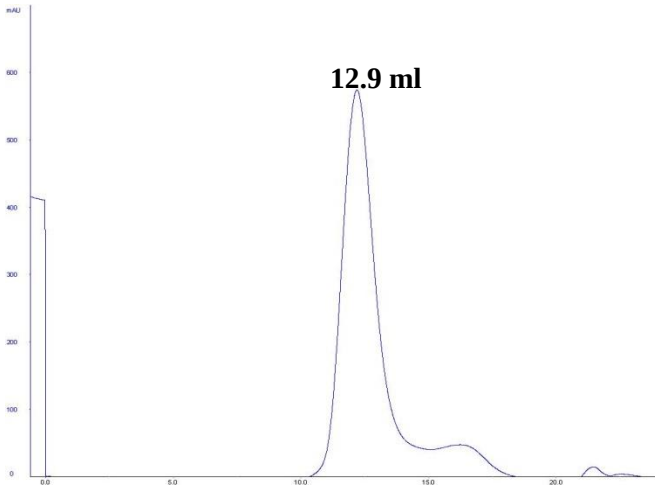

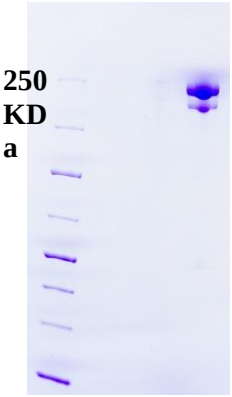

Superose 6

Talin full length T1767L, M319A, E1770K

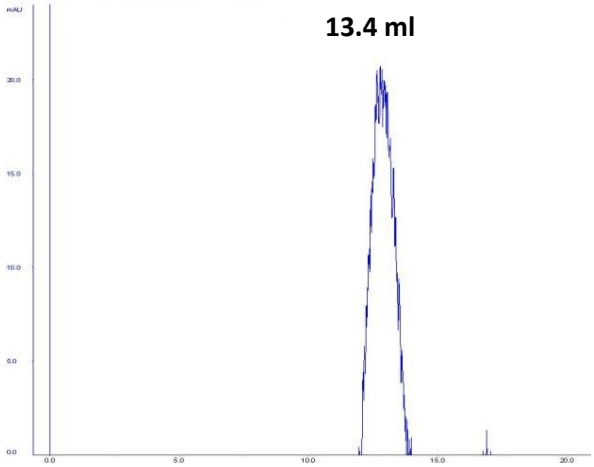

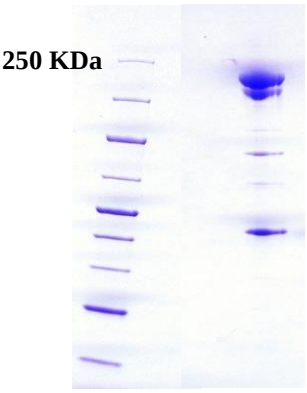

Superose 6

Biorad gel filtration standard (Superdex 200)

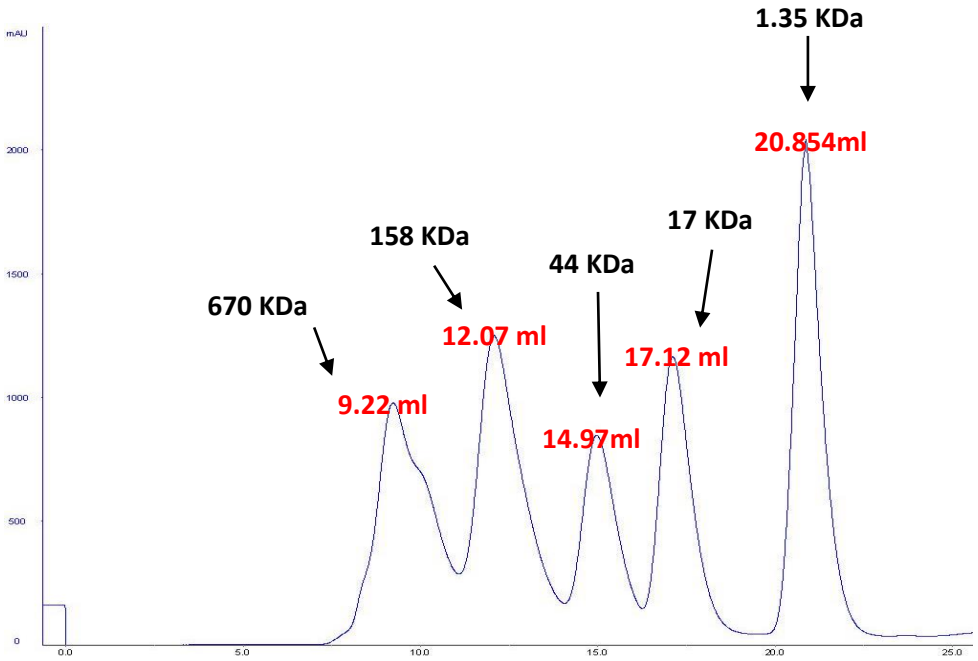

Biorad gel filtration standard (Superose 6)

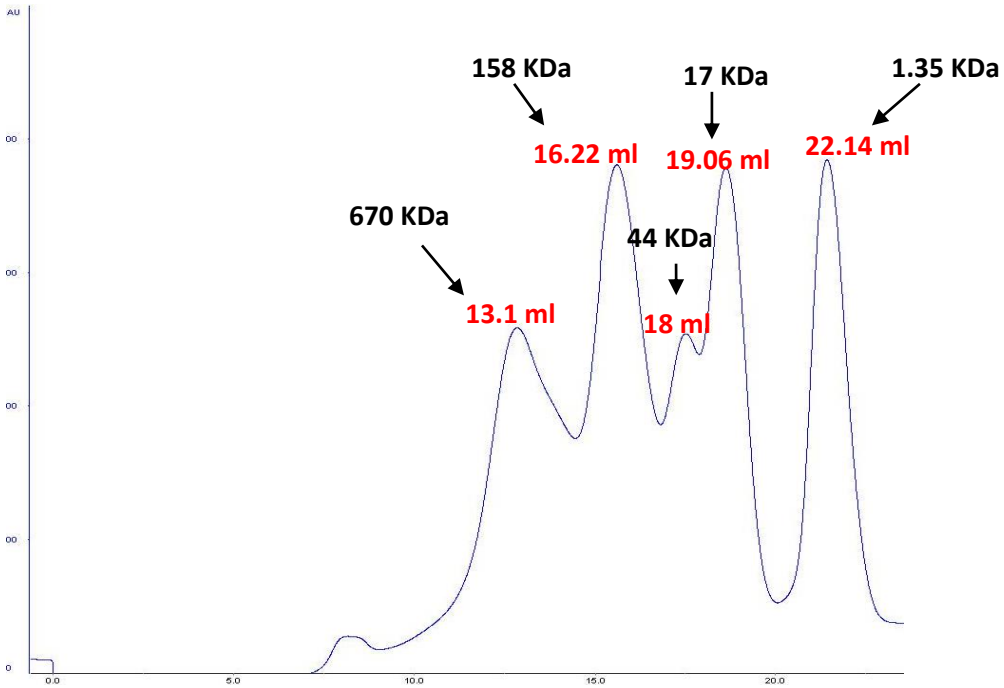

REFERENCES

1. Abram, C. L. and Lowell, C. A. (2009) The ins and outs of leukocyte integrin signalling. Annu. Rev. Immunol 27, 339–362.

2. Albiges-Rizo, C., Frachet, P. and Block, M. (1995) Down regulation of talin alters cell adhesion and the processing of the α5β1 integrin. Journal of Cell Science 108, 3317-3329.

3. Banno, A., Goult, B., Lee, H., Bate, N., Critchley, D. and Ginsberg, M. (2012) Subcellular Localization of Talin Is Regulated by Inter-domain Interactions. J. Biol. Chem. 287, 13799-13812.

4. Bass, M., Patel, B., Barsukov, I., Fillingham, I., Mason, R., Smith, B., Bagshaw, C., Critchley, D. (2002) Further characterization of the interaction between the cytoskeletal proteins talin and vinculin. Biochem. J. 362, 761-768.

5. Beckerle, M., Miller, D., Bertagnolli, M., Locke, S. (1989) Activation-dependent redistribution of the adhesion plaque protein, Talin, in intact human platelets. The Journal of Cell Biology 109, 3333-3346.

6. Begona Garcıa, A., Pereda , J., Calderwood, D., Ulmer, T., Critchley, D., Campbell, I., Ginsberg, M. and Liddington, R. (2003) Structural Determinants of Integrin Recognition by Talin. Molecular Cell 11, 49–58.

7. Berlin, C., Bargatze, R. F., Campbell, J. J., von Andrian, U. H., Szabo, M. C., Hasslen, S. R., Nelson, R. D., Berg, E. L., Erlandsen, S. L., and Butcher, E. C. (1995) Alpha 4 integrins mediate lymphocyte attachment androlling under physiologic flow. Cell 80, 413–422.

8. Bolton, S. , Barry, S., Mosley, H., Patel, B., Jockusch, B., Wilkinson, J. and Critchley D. (1997) Monoclonal Antibodies Recognizing the N- and C-Terminal Regions of Talin Disrupt Actin Stress Fibers When Microinjected Into Human Fibroblasts. Cell Motility and the Cytoskeleton 36, 363-376.

9. Brooks, P. C., Clark, R. A., and Cheresh, D. A. (1994) Requirement of vascular integrin alpha v beta 3 for angiogenesis Science 264, 569–57.

10. Brett, T., Legendre-Guillemin, V., McPherson, P. and Fremont, D. (2006) Structural definition of the F-actin-binding THATCH domain from HIP1R. Nature Structural & Molecular Biology. 13, 2.

11. Burridge, K., Mangeat, P. (1984) An interaction between vinculin and talin. Nature 308 (5961), 744-6.

12. Burridge, K., Connell, L. (1983) Talin: a cytoskeletal component concentrated in adhesion plaques and other sites of actin-membrane interaction. Cell Motil. 3(5-6), 405-17.

13. Borowsky, M. and Hynes, R. L. (1998) A Novel Talin-binding Transmembrane Protein Homologous with C-type Lectins, is Localized in Membrane Ruffles. The Journal of Cell Biology 143, 429–442.

14. Calderwood, D., Zent, R., Richard, G., Reesi, D., Hynes, R., and Ginsberg, M. (1999) The Talin Head domain binds to integrin β subunit cytoplasmic tails and regulates integrin activation. J. Biol. Chem 274, 28071-28074.

15. Calderwood, D., Yan, B., Pereda, J., Alvarez, B., Yosuke, F., Liddington R. and Ginsberg M. (2002) The Phosphotyrosine Binding-like Domain of Talin Activates Integrins. J. Biol. Chem. 277, 21749-21758.

16. Chen, H., Appeddu, P., Parsons, T., Hildebrand, J., Schaller, M. and Guan, J. (1995) Interaction of Focal Adhesion Kinase with cytoskeletal protein Talin. The Journal of Biological Chemistry 270, 16995-16999.

17. Delaglio, F., Grzesiek, S., Vuister, G. W., Zhu, G., Pfeifer, J, Bax, A. (1995) NMRPipe: a multidimensional spectral processing system based on UNIX pipes. J Biomol NMR 6, 277-293.

18. Fox, J. E., Goll, D. E., Reynolds, C. C., Phillips, D. R. (1985) Identification of two proteins (actin-binding protein and P235) that are hydrolyzed by endogenous Ca^{2+} dependent protease during platelet aggregation. J Biol Chem 260 (2), 1060-6.

19. Gingras, A., Bate, N., Goult, B., Hazelwood, L., Canestrelli, I., Grossmann, J., Liu, H., Putz, N., Roberts, G., Volkmann, N., Hanein, D., Barsukov, I. and Critchley, D. (2008) The structure of the C-terminal actin-binding domain of talin. The EMBO Journal 27, 458–469.

20. Goksoy, E., Ma, Y., Wang, X., Kong, X., Perera, D., Plow, E. and Qin, J. (2008) Structural basis for the autoinhibition of talin in regulating integrin activation. Mol Cell 31(1), 124-133.

21. Garrett, D. S., Powers, R., Gronenborn, A. M., Clore, G. M. (1991) A common-sense approach to peak picking in 2-dimensional, 3-dimensional, and 4-dimensional spectra using automatic computer-analysis of contour diagrams. J Magn Reson 95, 214-220.

22. Hemmings, L., Rees, D., Ohanian, V., Bolton, S., Gilmore, A., Patel, B., Priddle, H., Trevithick, J., Hynes, R. and Critchley, D. (1996) Talin contains three actin-binding sites each of which is adjacent to a vinculin-binding site. Journal of Cell Science 109, 2715-2726.

23. Huang, C., Zang, Q., Takagi, J., and Springer, T. A. (2000) Structural and functional studies with antibodies to the integrin beta 2 subunit. A model for the I-like domain. J. Bio. Chem. 275, 21514–21524.

24. Hynes, R.O. (2002) Integrins: bidirectional, allosteric signaling machines. Cell 110, 673-687.

25. Johnson, M. S., Lu, N., Denessiouk, K., Heino, J., and Gullberg, D. (2009) Integrins during evolution: evolutionary trees and model organisms. Biochim. Biophys. Acta. 1788, 779–789.

26. Kalli, A., Campbell, I., Sansom, M. (2013) Conformational Changes in Talin on Binding to Anionic Phospholipid Membranes Facilitate Signaling by Integrin Transmembrane Helices. PLoS Computational Biology. 9(10), e1003316.

27. Kim, M., Carman, C. V., and Springer, T. A. (2003) Bidirectional transmembrane signaling by cytoplasmic domain separation in integrins. Science 301, 1720–1725.

28. Ling, K., Doughman, R., Firestone, A., Bunce, M. and Anderson, R. (2002) Type Iγ phosphatidylinositol phosphate kinase targets and regulates focal adhesions. Nature 420.

29. Lee, W., Westler, W., Bahrami, A., Eghbalnia, H. R., Markley, J. L. (2009) PINE-SPARKY: graphical interface for evaluating automated probabilistic peak assignments in protein NMR spectroscopy. Bioinformatics 25, 2085-2087.

30. Lee, J. O., Rieu, P., Arnaout, M. A., and Liddington, R. (1995) Crystal structure of the A domain from the alpha subunit of integrin CR3 (CD11b/CD18). Cell 80, 631–638.

31. Lee, H., Bellin, R., Walker, D., Patel, B., Powers, P., Liu, H., Garcia-Alvarez, B., De Pereda, J., Liddington, R., Volkmann, N., Hanein, D., Critchley, D. And Robson, R. (2004) Characterization of an Actin-binding Site within the Talin FERM Domain. J. Mol. Biol. 343, 771–784.

32. Luo, B., Carman, C.., Springer, T. (2007) Structural basis of integrin regulation and signaling. Annu Rev Immunol 25, 619-647.

33. Luo, B., Takagi, J., and Springer, T. (2004) Locking the beta3 integrin I-like domain into high and low affinity conformations with disulfides. J. Biol. Chem. 279, 10215–10221.

34. Luo, B., Carman, C., Takagi, J., and Springer, T. (2005) Disrupting integrin transmembrane domain heterodimerization increases ligand binding affinity, not valency or clustering. Proc. Natl. Acad. Sci. USA 102, 3679–3684.

35. Ma, Y., Qin, J., Wu, C., and Plow, E. (2008) Kindlin-2 (Mig-2): a co-activator of β_3 integrins. J. Cell Biol. 181, 3439–446.

36. Ma, Y., Qin, J., Plow, E. (2007) Platelet integrin $\alpha_{IIb}\beta_3$: activation mechanisms. Journal of Thrombosis and Haemostasis 5, 1345-52.

37. Martel, V., Racaud-Sultan, C., Dupe, S., Marie, C., Frédérique, P., Galmiche, A., Block, M. and Albiges-Rizo, C. (2001) Conformation, Localization, and Integrin Binding of Talin Depend on Its Interaction with Phosphoinositides. J. Biol. Chem. 276, 21217-21227.

38. Muguruma, M., Matsumura, S. and Fukazawa, T. (1990) Direct interactions between Talin and actin. Biochemical and Biophysical Research Communications. 171, 1217-1223.

39. Monkley, S., Zhou, X., Kinston, S., Giblett, S., Hemmings, L., Priddle, H., Brown, J., Pritchard, C., Critchley, D., and Fassler, R. (2000) Disruption of the Talin Gene Arrests Mouse Development at the Gastrulation Stage. Developmental Dynamics 219, 560-574.

40. McCann, R. and Craig, S. (1997) The I/LWEQ module: a conserved sequence that signifies F-actin binding in functionally diverse proteins from yeast to mammals. Proc. Natl. Acad. Sci. USA 94, 5679–5684.

41. Moes, M., Rodius, S., Coleman, S. J., Monkley S. J., Goormaghtigh E., et al. (2007) The integrin binding site 2 (IBS 2) in the talin rod domain is essential for linking integrin beta subunits to the cytoskeleton. J. Biol. Chem. 282, 17280-88.

42. Borowsky M. and Hynes R. (1998) Layilin, A Novel Talin-binding Transmembrane Protein Homologous with C-type Lectins, is Localized in Membrane Ruffles. The Journal of Cell Biology 143, 429–442.

43. Paolo, G., Pellegrini, L., Letinic, K., Cestra, G., Zoncu, R., Voronov, S., Chang, S., Guo, J., Wenk, M. and Camilli, P. (2002) Recruitment and regulation of phosphatidylinositol phosphate kinase type 1g by the FERM domain of talin.. Nature 420.

44. Partridge, A. W., Liu, S., Kim, S., Bowie, J. U., and Ginsberg, M. H. (2005) Transmembrane domain helix packing stabilizes integrin alphaIIbbeta3 in the low affinity state. J. Biol. Chem. 280, 7294–7300.

45. Priddle, H., Hemmings, L., Monkley, S., Woods, A., Patel, B., Sutton, D., Dunn, G., Zicha, D., and Critchley, D. (1998) Disruption of the Talin Gene Compromises Focal Adhesion Assembly in Undifferentiated but Not Differentiated Embryonic Stem Cells. The Journal of Cell Biology 142, 1121-1133.

46. Qin, J., Vinogradova, O., Plow E. (2004) Integrin bidirectional signaling: a molecular view. PLoS Biol. 2, e169.

47. Schmidt, J., Zhang, J., Lee, H., Stromer, M., and Robson, R. (1999) Interaction of Talin with Actin: Sensitive Modulation of Filament Crosslinking Activity. Archives of Biochemistry and Biophysics. 366, 139–150.

48. Shi, M., Sundramurthy, K., Liu, B., Tan, S. M., Law, S. K., and Lescar, J. (2005) The crystal structure of the plexin-semaphorin-integrin domain/hybrid domain/I-EGF1 segment from the human integrin beta2 subunit at 1.8-A resolution. J. Biol. Chem. 280, 30586–30593.

49. Springer, T. A. (1997) Folding of the N-terminal, ligand-binding region of integrin alpha-subunits into a beta-propeller domain. Proc. Natl. Acad. Sci. USA. 94, 65–72.

50. Song, X., Yang, J., Hirbawi, J., Ye, S., Perera, D., Goksoy, E., Dwivedi, P., Plow, E., Zhang, R., Qin, J. (2012) A novel membrane-dependent on/off switch mechanism of talin FERM domain at sites of cell adhesion. Cell Research. 22, 1533-1545.

51. Sun, N., Critchley, D., Paulinc, D., Lid, Z., Robsona, R. (2008) Identification of a repeated domain within mammalian α-synemin that interacts directly with talin. Experimental Cell Research 314, 1839-1849.

52. Tidball, J. G, O'Halloran, T., Burridge. (1986) Talin at myotendinous junctions. J Cell Biol. 103 (4), 1465-72.

53. Takagi, J., Petre, B. M.., Walz, T., and Springer, T. A. (2002) Global conformational rearrangements in integrin extracellular domains in outside-in and inside-out signaling. Cell 110, 599–511.

54. Ulmer, T. S., Calderwood, D. A., Ginsberg, M. H., Campbell, I. D. (2003) Domain specific interactions of talin with the membrane-proximal region of the integrin beta3 subunit. Biochemistry 42, 8307–12.

55. Vinogradova, O., Velyvis, A., Velyviene, A., Hu, B., Haas, T., Plow, E. F., and Qin, J. (2002) A structural mechanism of integrin αIIbβ3 'inside-out' activation as regulated by its cytoplasmic face. Cell 110, 587-597.

56. Vinogradova, O., Vaynberg, J., Kong, X., Haas, T.A., Plow, E.F. Qin, J. (2004) Membrane-mediated structural transitions at the cytoplasmic face during integrin activation. Proc. Natl. Acad. Sci 101, 4094-9.

57. Xiong, J. P., Stehle, T., Diefenbach, B., Zhang, R., Dunker, R., Scott, D. L., Joachimiak, A., Goodman, S. L., and Arnaout, M. A. (2001) Crystal structure of the extracellular segment of integrin alphaVbeta3. Science 294, 339–345.

58. Xiong, J. P., Stehle, T., Zhang, R., Joachimiak, A., Frech, M., Goodman, S. L., and Arnaout, M. A. (2002) Crystal structure of the extracellular segment of integrin alpha Vbeta3 in complex with an Arg-Gly-Asp ligand. Science 296, 151–155.

59. Xiao, T., Takagi, J., Coller, B. S., Wang, J. H., and Springer, T. A. (2004) Structural basis for allostery in integrins and binding to fibrinogen- mimetic therapeutics. Nature 432, 59–67.

60. Zhu, J., Luo, B. H., Xiao, T., Zhang, C., Nishida, N., and Springer, T. A. (2008) Structure of a complete integrin ectodomain in a physiologic resting state and activation and deactivation by applied forces. Mol. Cell 32, 849–861.

61. Zhu, J., Luo, B. H., Barth, P., Schonbrun, J., Baker, D., and Springer, T. A. (2009) The structure of a receptor with two associating transmembrane domains on the cell surface: integrin alphaIIbbeta3. Mol. Cell 34, 234–249.